FMRP-Regulated RNA Splicing is Mediated by Multiple Splicing Factors and Translational Control of *Mbnl1* RNA

Suna Jung[1], Sneha Shah[1], and Joel D. Richter[2]

Program in Molecular Medicine

University of Massachusetts Chan Medical School

Worcester MA 01605 USA

[1]equal contributors

[2]corresponding author. joel.richter@umassmed.edu

Key words: FMRP, Fragile X Syndrome, Alternative splicing, MBNL1, PTBP1, hnRNPF, hnRNPQ

Running title: FMRP regulation of splicing

Abstract

The neurodevelopmental disorder Fragile X Syndrome (FXS) is often modeled in *Fmr1* knockout mice, which results in the loss of the RNA binding protein FMRP. In the brain, FMRP stalls ribosomes on specific mRNAs including *Setd2,* whose encoded protein catalyzes the epigenetic mark H3K36me3. In the absence of FMRP, SETD2 levels are excessive, which alters the H3K36me3 landscape and secondarily, alternative pre-mRNA splicing. Here we show that in *Fmr1*-deficient mice, RNA mis-splicing occurs in several brain regions and peripheral tissues. To assess molecular mechanisms of splicing mis-regulation, we employed N2A cells depleted of *Fmr1*. In the absence of FMRP, RNA-specific exon skipping events are linked to the splicing factors hnRNPF, hnRNPQ, PTPB1, and MBNL1. FMRP binds to *Mbnl1* mRNA and regulates its translation. In *Fmr1*-depleted cells, *Mbnl1* RNA itself is mis-spliced, which results in the loss of a nuclear localization signal (NLS)-containing exon that in turn alters the nucleus-to-cytoplasm ratio of MBNL1. This re-distribution of MBNL1 isoforms in *Fmr1*-deficient cells likely results in splicing changes in other RNAs. *Mbnl1* mis-spicing also occurs in human FXS post-mortem brain. These data link FMRP-dependant impaired translation of splicing factors, such as MBNL1, to altered self-splicing and subcellular localization of the *Mbnl1* RNA and protein. Altered expression of splicing factors in the absence of FMRP may cascade into the global dys-regulation of tissue specific splicing observed in *Fmr1* deficient cells.

Introduction

Fragile X Syndrome (FXS) is a neuro-developmental disorder characterized by mild to severe intellectual disability, speech and developmental delays, social impairment, perseveration, aggression, anxiety, and other maladies. FXS lies on the autism spectrum and is the most common single gene cause of autism. FXS is caused by an expansion of 200 or more CGG triplets in the 5' untranslated region (UTR) of *FMR1*, which in turn induces DNA methylation and gene silencing. Loss of the *FMR1* gene product FMRP results in the disruption of neuronal circuitry and synaptic efficacy, which produces an array of neuro-pathological conditions (Santoro et al 2012; Hagerman et al 2017; Richter and Zhao 2021). FMRP, an RNA binding protein present in probably all cells is frequently studied in mouse hippocampus, where several studies show that it represses protein synthesis (Dölen et al 2007, Darnell et al 2011; Osterweil et al 2013, Udagawa et al 2013). This observation, in conjunction with results showing that FMRP co-sediments with polysomes in sucrose gradients (Feng et al 1997; Stefani et al 2004) and that it UV CLIPs (crosslink-immunoprecipitation) mostly to coding regions of mRNA (Darnell et al 2011; Maurin et al 2018; Sawicka et al 2019; Li et al 2020), suggested that it inhibits translation by impeding ribosome translocation. Indeed, it is now clear that at least one activity of FMRP is to stall ribosomes (Darnell 2011; Udagawa et al 2013; El Fatimy et al 2016; Das Sharma et al 2019; Shah et al 2020). How this occurs is unclear, but it could involve codon bias or optimality (Shu et al 2020; Richter and Coller 2015), impairment of ribosome function (Chen et al 2014), or formation of translationally quiescent subcellular granules (El Fatimy et al 2016).

One group of FMRP target RNAs encodes chromatin modifying enzymes (Darnell et al 2011; Korb et al 2017; Hale et al 2021). The synthesis of several of these enzymes is inhibited by FMRP; in its absence, excessive levels of these chromatin proteins alter the epigenetic landscape, which in turn impairs cognitive function (Korb et al 2017). A few mRNAs encoding epigenetic factors

associate with FMRP-stalled ribosomes (Shah et al 2020). One of these, *Setd2*, encodes an enzyme that establishes the histone modification H3K36me3, which is most often located in gene bodies (Schwartz et al. 2009; Kolasinska-Zwierz et al 2009). In *Fmr1*-deficient mouse brain, SETD2 protein levels are elevated, which in turn alter the distribution of H3K36me3 chromatin marks. H3K36me3 has been linked to alternative pre-mRNA splicing (Kim et al 2011; Pradeepa et al 2012; Bhattacharya et al 2021), and indeed there is some correlation between the genes with recast H3K36me3 and altered splicing in *Fmr1*-deficient mouse hippocampus (Shah et al 2020). The observation that *Fmr1*-deficiency results in hundreds of mis-splicing events prompted us to investigate both the prevalence and mechanism of FMRP-regulated nuclear pre-RNA processing.

We find that mis-splicing, mostly exon skipping, is widespread in *Fmr1*-deficient mice and occurs in all brain regions and peripheral tissues examined. To determine how FMRP might regulate splicing, we depleted *Fmr1* from mouse N2A cells, which resulted in hundreds of mis-splicing events. We focused on specific exons in three RNAs that are aberrantly skipped or included in *Fmr1*-deficient cells and mapped surrounding splicing factor consensus binding sites. Splicing factors MBNL1, PTBP1, and hnRNPF are responsible for altered splicing in *Fmr1*-deficient cells. FMRP binds to *Mbnl1* and *Ptbp1* mRNA and also regulates the translation of two of these factors, MBNL1 and hnRNPQ. Moreover, *Mbnl1* RNA itself undergoes alternative splicing, which is impaired in *Fmr1*-deficient cells. In the absence of FMRP, an NLS-containing exon is frequently skipped, which alters the nucleus-cytoplasm distribution of MBNL1. This change in subcellular localization of MBNL1 likely affects splicing decisions on other mRNAs. In addition, *Mbnl1* splicing is altered in human FXS post-mortem cortex, suggesting that it could modify the brain proteome and thereby contribute to intellectual impairment and Fragile X Syndrome.

97 ## Results

98

99 ### RNA splicing mis-regulation in *Fmr1* KO brain

100 Gene expression and RNA splicing are mis-regulated in the *Fmr1*-deficient mouse hippocampus
101 (Shah et al 2020). To determine whether this mis-regulation occurs in other brain regions and in
102 peripheral tissues, we sequenced RNA from (n=3, 2-3 month old) WT and *Fmr1* KO hippocampus,
103 cerebellum, and cortex, as well as liver, muscle, and testis (**Figure 1A**). Volcano plots show that
104 hundreds of RNAs are up or down-regulated in *Fmr1* KO cortex although fewer RNAs were
105 similarly mis-regulated in hippocampus and cerebellum (log2FC, FDR < 0.05, n=3) (**Figure 1B;**
106 **Supplementary file 1**). A Venn diagram shows that a significant group of RNAs, mostly encoding
107 proteins involved in synapse or cell junction formation, was shared between hippocampus and
108 cortex (**Figure 1C**). In the cortex, many upregulated RNAs encode proteins involved in RNA
109 processing for biogenesis, while down regulated RNAs code for proteins mediating membrane
110 potential and synapse organization (**Figure 1D**). Analysis of these RNA seq datasets
111 demonstrates that hundreds of RNAs are mis-spliced, mostly exon skipping, in the *Fmr1*-deficient
112 hippocampus, cortex, and cerebellum (log2FC, FDR < 0.05, Percent spliced-in [PSI] > 0.05, n=3)
113 (**Figure 1E; Supplementary file 2-4**). For the hippocampus and cortex, the percent of exons
114 spliced in has a median of about 20% **Figure 1F**)**.** In the cortex and hippocampus, RNAs
115 displaying differential exon skipping between the two genotypes encode proteins involved in
116 synapse organization and development and JNK signaling, respectively (**Figure 1- figure**
117 **supplement 1A**). **Figure 1G** shows RT-PCR confirmation of exon 6 skipping of Defective in Cullin
118 Neddylation 1d2 (*Dcun1d2*) RNA. In both brain regions there was a > 2-fold increase in exon 6
119 skipping upon *Fmr1* deficiency compared to wild type (WT). Similar levels of the *Dcun1d2*
120 constitutive exon 2 served as an internal control suggesting no change in *Dcun1d2* total RNA
121 levels in the *Fmr1* KO tissues.

122

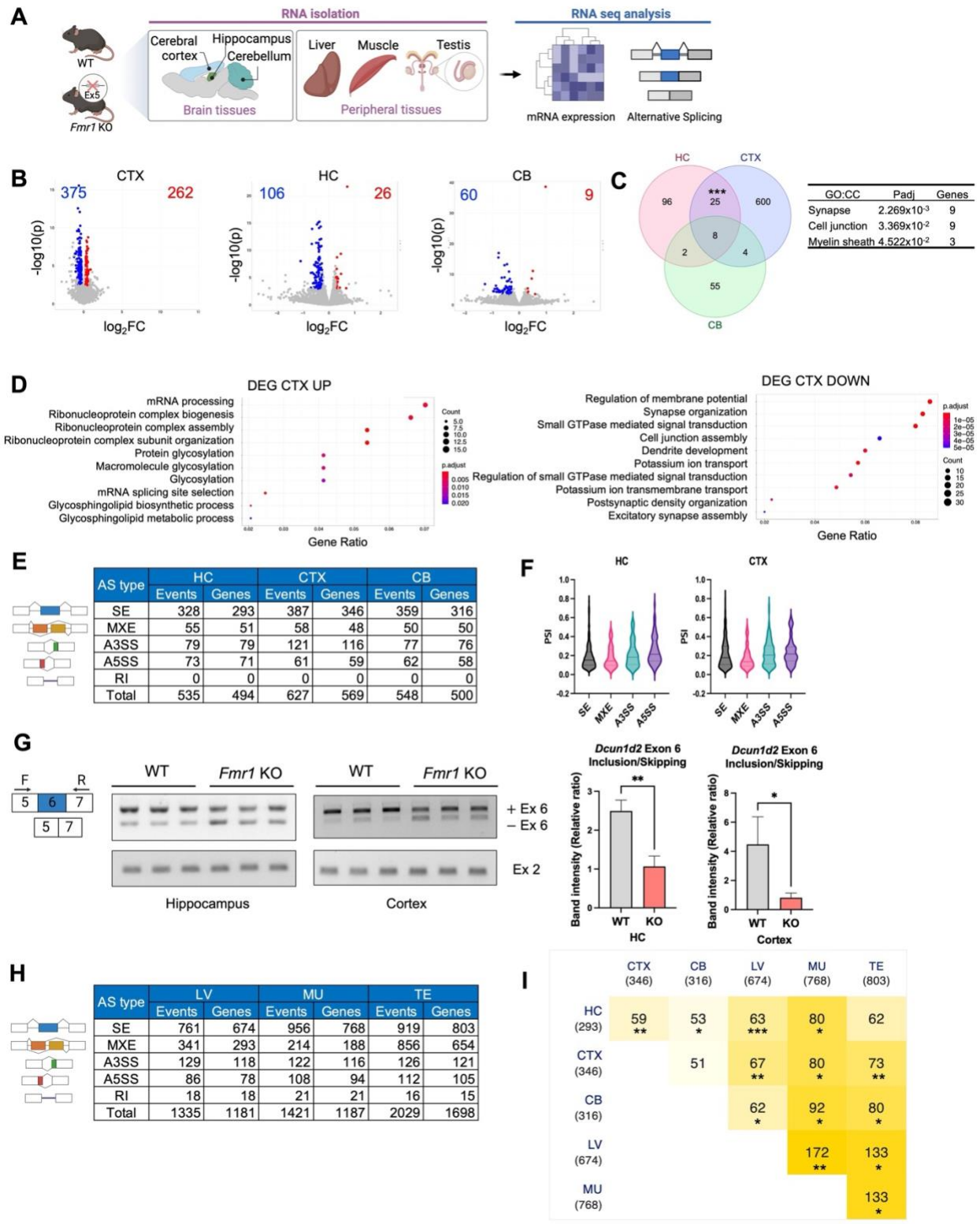

AS type	HC		CTX		CB	
	Events	Genes	Events	Genes	Events	Genes
SE	328	293	387	346	359	316
MXE	55	51	58	48	50	50
A3SS	79	79	121	116	77	76
A5SS	73	71	61	59	62	58
RI	0	0	0	0	0	0
Total	535	494	627	569	548	500

AS type	LV		MU		TE	
	Events	Genes	Events	Genes	Events	Genes
SE	761	674	956	768	919	803
MXE	341	293	214	188	856	654
A3SS	129	118	122	116	126	121
A5SS	86	78	108	94	112	105
RI	18	18	21	21	16	15
Total	1335	1181	1421	1187	2029	1698

Figure 1. Differential gene expression in *Fmr1*-deficient brain and peripheral tissues.

(A) Schematic of analysis. Created with BioRender.com.

(B) Volcano plots of differential gene expression comparing WT and *Fmr1*-deficient cortex (CTX), hippocampus, HC), and cerebellum (CB). The numbers refer to those RNAs that are up or down-regulated between the two genotypes (n=3, FDR < 0.05).

(C) Venn diagram comparing differential RNA levels from WT and *Fmr1* KO hippocampus, cortex, and cerebellum (hypergeometric test, ***p < 0.001). GO terms for cellular components and p-value for overlaped RNAs are indicated.

(D) GO terms for RNAs that are significantly up or down regulated in the cortex.

(E) Changes in alternative RNA splicing (SE, skipped exons; MXE, mutually exclusive exons; A3SS, alternative 3' splice site; A5SS, alternative 5' splice site; RI, retained intron) in *Fmr1* KO HC, CTX, or CB relative to WT (log2FC, p < 0.05, n=3).

(F) Percent spliced in (PSI) distribution for HC and CTX. The solid line is the median and the dashed lines are quartiles. p-value < 0.05, PSI > 0.05.

(G) RT-PCR validation of altered *Dcun1d2* exon 6 inclusion/skipping in *Fmr1* KO HC and CTX. *Dcun1d2* constitutive Exon 2 was amplified to compare total mRNA levels between the genotypes and mean ± S.D is shown (Student's t-test, *p < 0.05, **p < 0.01).

(H) Changes in alternative RNA splicing events (SE, skipped exons; MXE, mutually exclusive exons; A3SS, alternative 3' splice site; A5SS, alternative 5' splice site; RI, retained intron) in *Fmr1* KO liver (LV), muscle (MU), and testis (TE) relative to WT (PSI > 0.05, p < 0.05, n=3).

(I) Comparison of all exon skipping changes in *Fmr1* brain regions and peripheral tissues relative to WT (hypergeometric test, *p < 0.05; **p < 0.01; ***p < 0.001).

Aberrant RNA splicing in *Fmr1* KO peripheral tissues

Because FMRP is expressed in probably all tissues, we examined RNA splicing in WT and *Fmr1* deficient liver, muscle (gastrocnemius), and testis. As with the brain, hundreds of RNAs are up or down regulated in FMRP KO peripheral tissues relative to WT (FDR, p < 0.05, n=3) (**Figure 1-figure supplement 1B; Supplementary file 1**), which may be somewhat surprising because

relative *Fmr1* levels (in transcripts per million, TPM) in these tissues are about one-tenth the amount in the brain (**Figure 1-figure supplement 1C**). In the liver, RNAs that are up or down regulated in FMRP KO relative to WT encode factors involved in various metabolic processes and catabolic and phosphorylation events, respectively (**Figure 1-figure supplement 1D**). In muscle, up or down regulated RNAs encode factors involved in extra cellular matrix organization and mitochondrial function, respectively (**Figure 1-figure supplement 1E**). In testis, up or down regulated RNAs encode factors involved in cell division, and reproductive system development, respectively (**Figure 1-figure supplement 1F**).

In FMRP KO peripheral tissues, splicing mis-regulation is widespread, as in the brain mostly skipped exons but a large number of mutually exclusive exons as well (log2FC $p < 0.05$, PSI > 0.05, n=3) (**Figure 1H; Supplementary file 5-7**). In the liver and muscle, RNAs with differential exon skipping between the two genotypes encode chromatin modifying enzymes and Wnt signaling components, respectively (**Figure 1-figure supplement 1G**). Comparison of the RNAs from all brain regions and peripheral tissues that display significantly different exon skipping between the two genotypes shows a remarkable degree of overlap **Figure 1I**). For example, nearly 20% of RNAs with skipped exons in hippocampus are the same as in cortex, which might be expected. However, ~10% of RNAs with skipped exons in the liver also exhibit exon skipping in the hippocampus. In this same vein, ~9% of RNAs with skipped exons in the testis also show exon skipping in the cortex. These data indicate that if FMRP regulates exon skipping in one type of tissue (e.g., the brain), it is likely to do so in another tissue (e.g., liver).

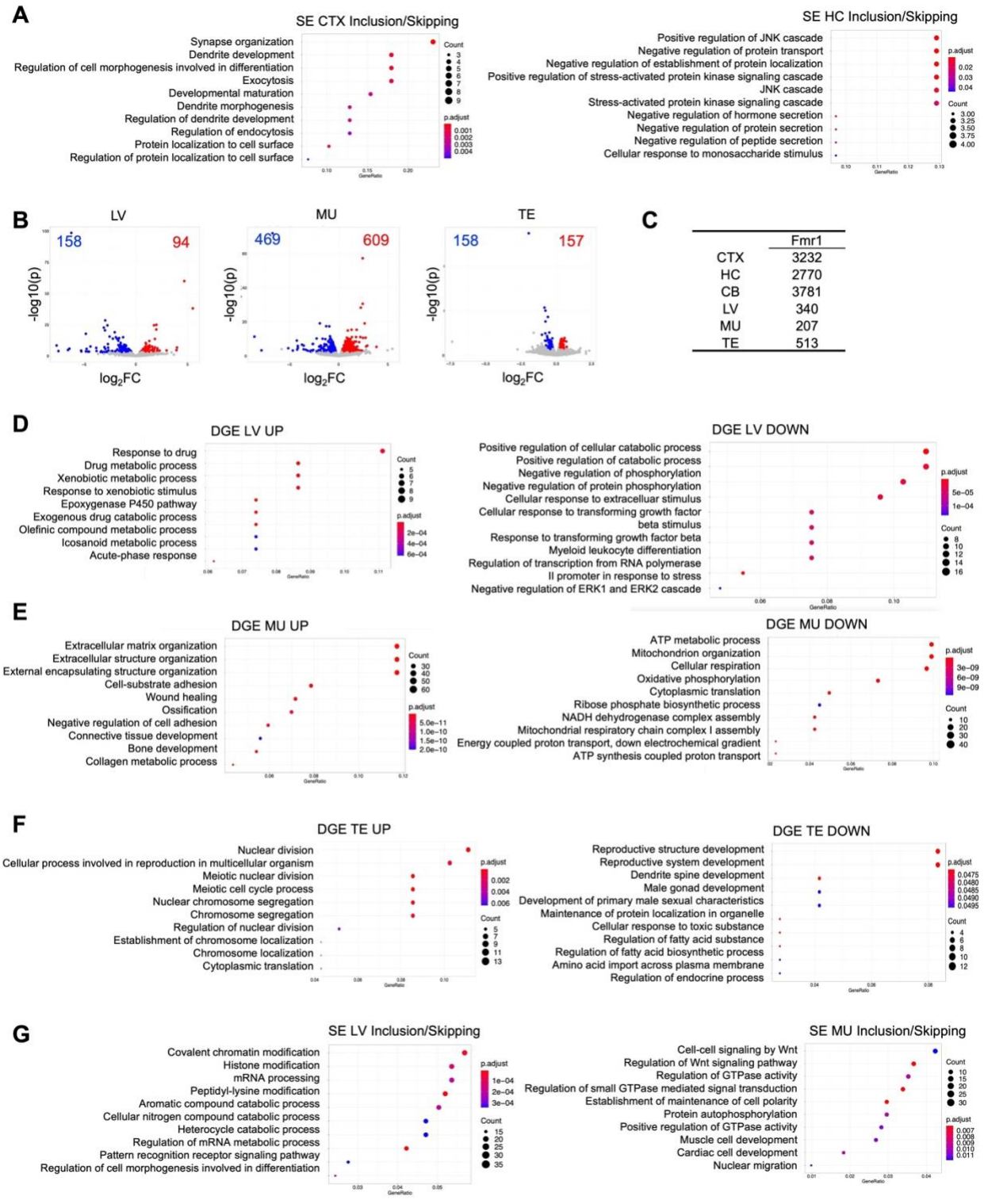

Figure 1 – figure supplement 1. Gene Ontology (GO) terms.

(A) GO terms for skipped/included exons in *Fmr1* KO CTX and HC.

(B) Volcano plots of RNAs up or down regulated (log2FC, FDR < 0.05, n=3) in *Fmr1* KO liver (LV), muscle (MU), and testis (TE).

(C) *Fmr1* RNA levels (TPM) in brain regions and peripheral tissues.

(D-F) GO terms of RNAs up or down regulated in *Fmr1* KO liver, muscle, and testis,

(G) GO terms for skipped/included exons in *Fmr1* KO liver and muscle.

FMRP-regulated splicing in N2A cells

To investigate the mechanism of FMRP-mediated splicing, we surmised that using a single cell type would be a more efficacious approach compared to a tissue containing multiple cell types. Consequently, we used mouse N2A neuroblastoma cells depleted of *Fmr1* by an siRNA complementary to this RNA's 3'UTR, which reduced FMRP levels by > 95% compared to a nontargeting (NT) control (**Figure 2A**). We next performed RNA-seq from cells transfected with either the nontargeting or *Fmr1* targeting siRNAs. **Figure 2B** and **Figure 2 - figure supplement 1A** shows that there were ~2000 RNAs that were mis-spliced (log2FC, p < 0.05, PSI > 0.05, **Supplementary file 8**). Several of these mis-splicing events were validated by RT-PCR: *Mapt* (microtubule associated protein tau) exon 4, *Tnik* (TRAF2 and NCK interacting kinase*)* exon 21, and *Wnk1* (WNK Lysine Deficient Protein Kinase 1) exon 11 were all included more in *Fmr1* depleted cells compared to nondepleted cells while *App* (amyloid precursor protein) exon 8, *Ski* (SKI protooncogene) exon 2, and *Os9* (Osteosarcoma Amplified 9, endoplasmic reticulum lectin) exon 13 were all skipped in *Fmr1*-depleted cells relative to non-depleted cells (**Figure 2C**).

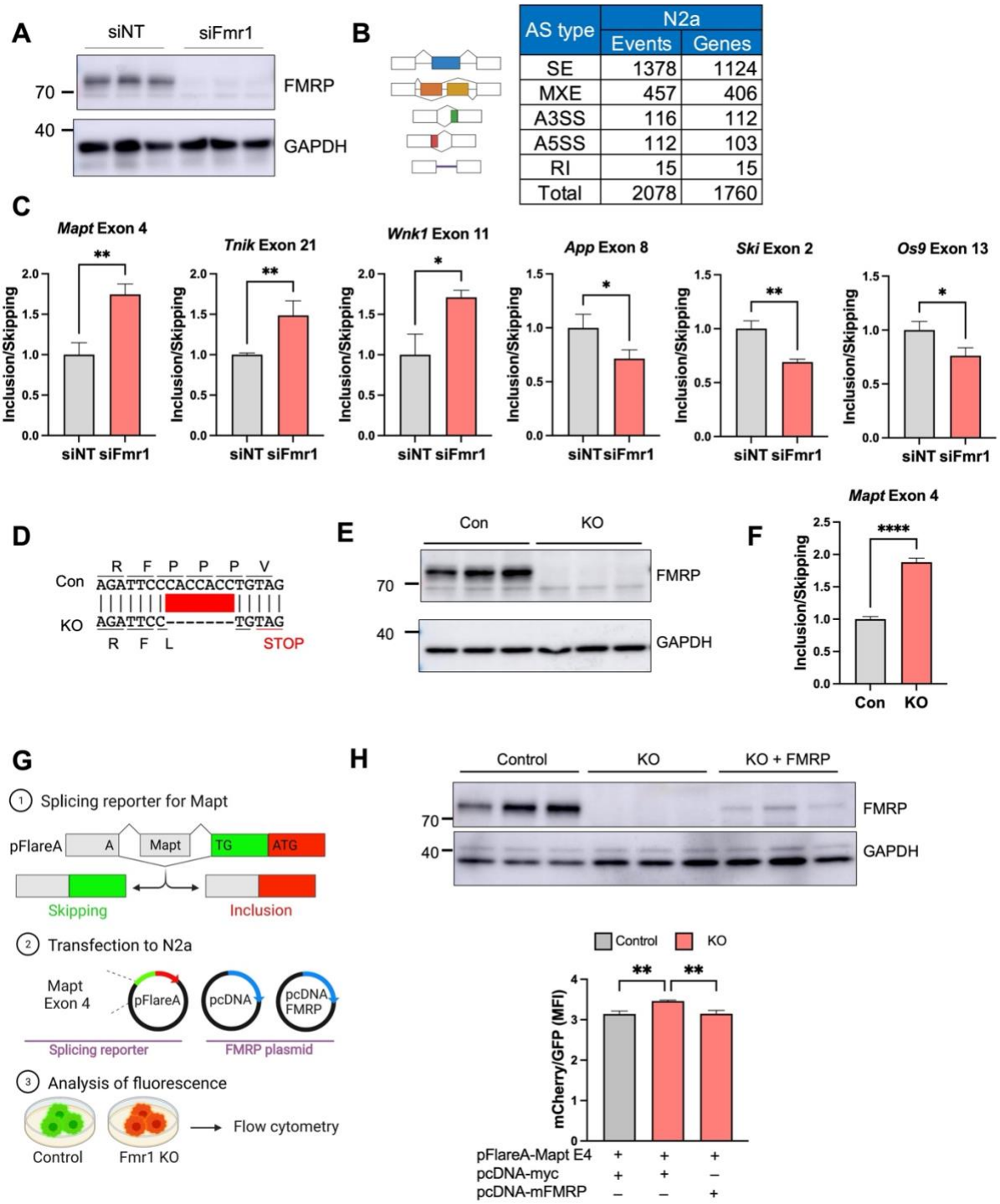

AS type	N2a	
	Events	Genes
SE	1378	1124
MXE	457	406
A3SS	116	112
A5SS	112	103
RI	15	15
Total	2078	1760

Figure 2. Mis-regulated splicing in *Fmr1*-deficient mouse N2A neuroblastoma cells. (A) Western blots showing depletion of FMRP following siRNA knockdown of *Fmr1*. GAPDH serves as a loading control. siNT refers to a nontargeting siRNA control.

(B) Types of mis-splicing events and the number of genes affected in *Fmr1*-depleted N2A cells (PSI > 0.05; p < 0.05; n=2 for siNT, n=3 for siFmr1).

(C) qPCR validation of mis-splicing events (exons skipped or included) in six RNAs in *Fmr1*-depleted cells compared to siNT control (Student's t-test, n=3: *p < 0.05; **p < 0.01). Mean ± S.D is shown.

(D) CRISPR/Cas9-edited portion of *Fmr1***,** which deletes seven nucleotides leading to a frame-shift and nonsense-mediated RNA decay.

(E) Western blot of FMRP in control and *Fmr1*-edited cells.

(F) qPCR of *Mapt* exon 4 skipping/inclusion in *Fmr1*-edited cells compared to control and mean ± S.D is shown (Student's t-test, ****p < 0.0001).

(G) pFlare system for assessing exon skipping and inclusion. *Mapt* exon 4 was inserted into pFlareA. When the exon is skipped, GFP is expressed; when the exon is included, RFP is expressed. This plasmid, as well as an empty pcDNA plasmid or one that expresses mouse FMRP, was transfected into control or *Fmr1* KO N2A cells. The cells were then analyzed by flow cytometry. Created with BioRender.com.

(H) Western blot of FMRP from control cells, CRISP/Cas9-edited cells transduced with empty pcDNA, and CRISPR/Cas9-edited cells transduced with pcDNA FMRP. The histogram quantifies the ratio of cells expressing GFP or mCherry and mean ± S.D is shown (one-way ANOVA, **p < 0.05, n=3).

Rescue of mis-regulated splicing by FMRP replacement

To confirm FMRP control of splicing by an entirely different method, we used CRISPR/Cas9 gene editing to delete 7 nucleotides from exon 3 of *Fmr1*, which causes a reading frame shift to a stop codon resulting in nonsense mediated mRNA decay (**Figure 2D; Figure 2 - figure supplement 1B**) and a complete loss of FMRP (**Figure 2E**). In these KO cells, loss of *Mapt* exon 4 skipping was nearly identical as observed with siFmr1 knockdown of *Fmr1* (**Figure 2F**). We next generated

a reporter construct where *Mapt* exon 4 and its flanking intron sequences were inserted into the pFlareA plasmid, which contains GFP and RFP sequences. Here, if *Mapt* exon 4 is included, an A nucleotide will generate a start codon when juxtaposed to a TG dinucleotide following splicing to the RFP reading frame and will express RFP. If Mapt exon 4 is skipped, GFP will be expressed (**Figure 2G**). This plasmid, together with an FMRP-expressing plasmid or an empty control plasmid, were transfected into normal or *Fmr1* KO N2A cells and green/red fluorescence intensity was analyzed by flow cytometry (**Figure 2G**). The western blot in **Figure 2H** shows the expression level of FMRP relative to GAPDH. The "rescuing" ectopic FMRP was expressed at ~10% of endogenous FMRP levels. In the FMRP KO cells, *Mapt* exon 4 in the reporter was more included relative to that observed in control cells, which replicates the data with endogenous *Mapt* exon 4 with both siFmr1 depletion (**Figure 2C**) and CRISPR/Cas9-edited *Fmr1* KO cells (**Figure 2F**), albeit not to the same extent. Importantly, ectopic expression of FMRP in the KO cells restored *Mapt* exon 4 inclusion to control cells levels, demonstrating the reversibility of the exon skipping that is FMRP-dependent.

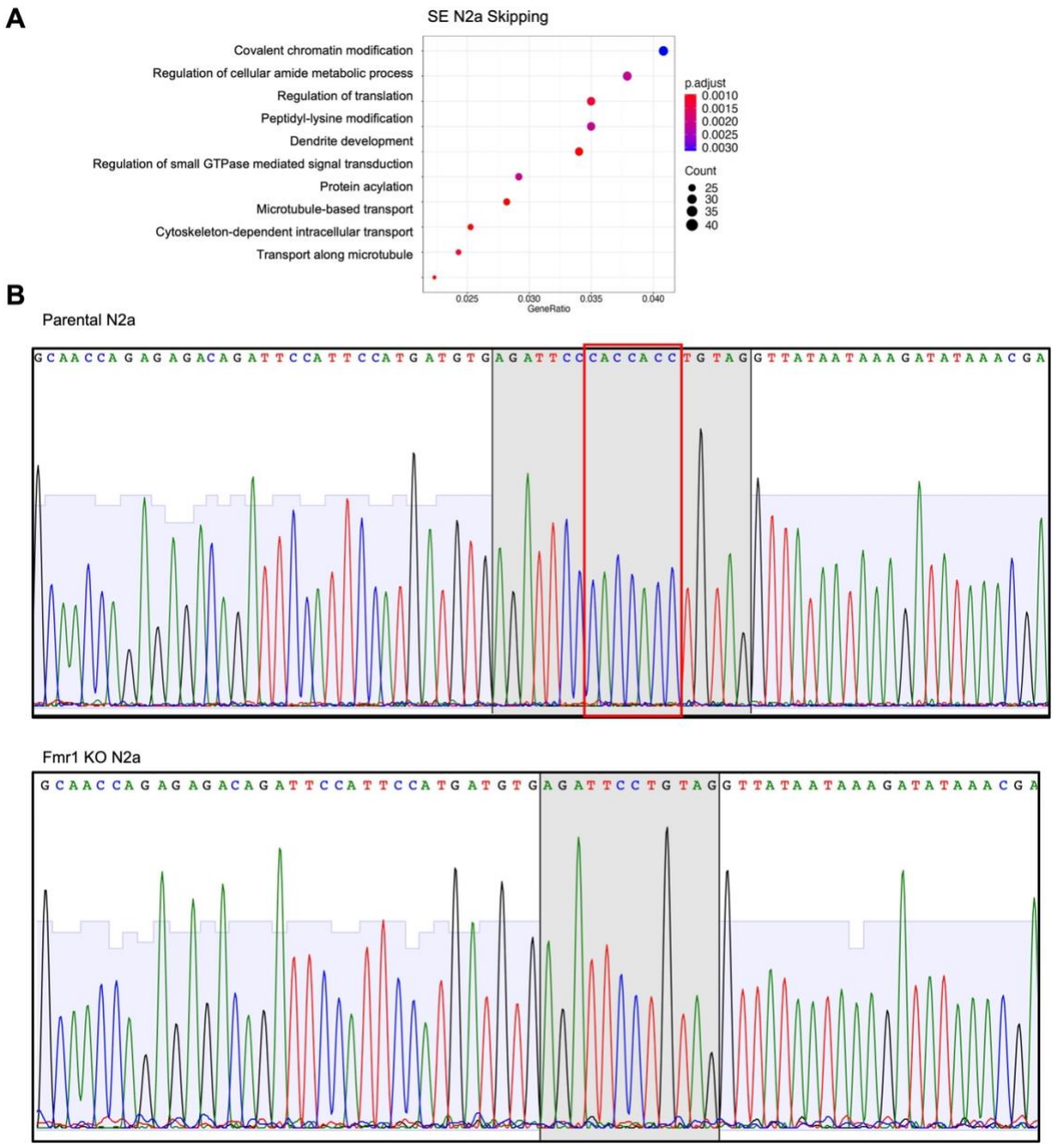

Figure 2 – figure supplement 1.

(A) GO terms for RNAs that display exon skipping in *Fmr1*-depleted N2A cells.

(B) DNA sequence analysis of parental N2A cells (top) and Fmr1-depleted cells (bottom). The shaded portion corresponds the amino acid sequences shown in **Figure 2**. The red box indicates the nucleotides depleted by CRISPR/Cas9 editing. Following editing, the TAG at the right of the shaded box becomes a premature stop codon, leading to nonsense mediated mRNA decay and loss of FMRP expression.

FMRP regulation of splicing factor activity

To identify splicing factors that might be regulated by FMRP, we focused on exons in three RNAs that are skipped or included in *Fmr1*-deficient cells and used the SFMap database (Akerman et al 2009) to identify potential splicing factor binding sites. *Mapt* exon 4, which is more included in *Fmr1*-deficient cells relative to control cells, is flanked by binding sites for splicing factors MBNL1, PTBP1, hnRNPF, and hnRNPQ (**Figure 3A**). We depleted the RNAs encoding each of these splicing factors as well as *Fmr1* (**Figure 3- figure supplement 1A-H**). Depletion of *Mbnl1* resulted inclusion of exon 4 even more so compared to *Fmr1* depletion. A double depletion of both *Mbnl1* and *Fmr1* caused even greater exon inclusion than the single depletions (**Figure 3B**). Constitutive *Mapt4* exon 15 was unaffected by these depletions (**Figure 3- figure supplement 1I)**. Depletion of *Ptbp1* also resulted in a greater inclusion of *Mapt* exon 4 than *Fmr1* depletion. A double *Fmr1/Ptbp1* depletion was similar to *Fmr1* depletion alone (**Figure 3B; Figure 3- figure supplement 1J**). Depletion of hnRNPF or hnRNPQ had no effect on *Mapt* exon 4 skipping/inclusion (**Figure 3B; Figure 3B, Figure 3- figure supplement 1K,L**). Because the magnitude of *Mapt* exon 4 inclusion was additive when both *Mbnl1* and *Fmr1* were depleted, we surmise that a second splicing factor under the control of FMRP is involved in this splicing event.

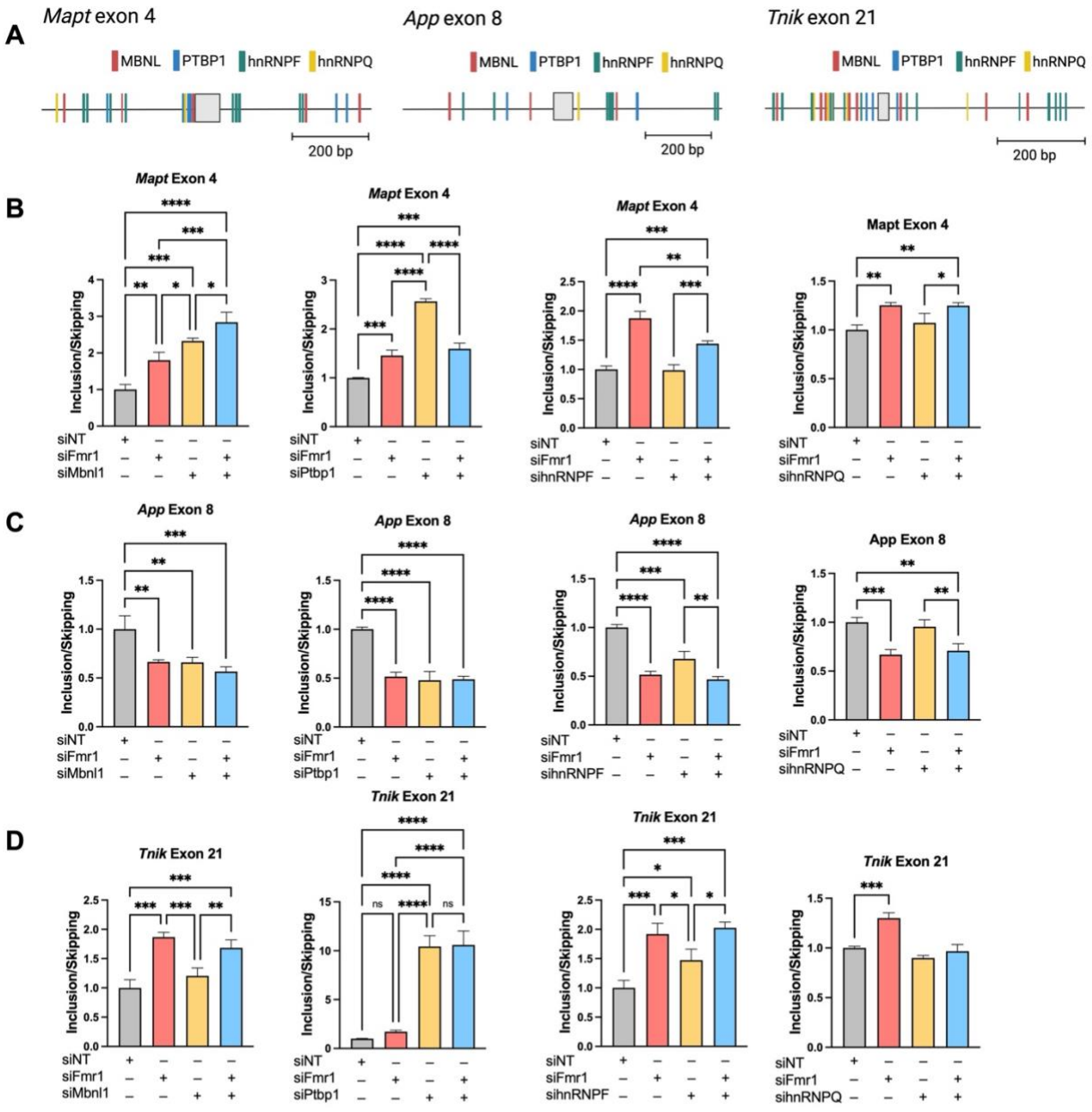

E

		Inclusion/Skipping		
		Mapt Exon 4	*Tnik* Exon 21	*App* Exon 8
Single knockdown	*Fmr1*	1.70	1.60	0.59
	Mbnl1	2.32	1.20	0.66
	Ptbp1	2.57	9.16	0.48
	hnRNPF	1.10	1.47	0.68
	hnRNPQ	1.07	0.90	0.95
Double knockdown	*Fmr1/Mbnl1*	3.84	1.68	0.57
	Fmr1/Ptbp1	1.59	9.99	0.49
	Fmr1/hnRNPF	1.77	2.03	0.47
	Fmr1/hnRNPQ	1.25	0.97	0.71

Figure 3. RNA binding proteins control specific splicing events in *Fmr1*-depleted N2A cells.

(A) Consensus binding motifs of hnRNPF, hnRNPQ, MBNL1, and PTPBP1 flanking skipped or included exons of *Mapt* (exon 4), *App* (exon 8), and *Tnik* (exon21) RNAs. Created with SFmap and Biorender.com.

(B) FMRP-dependent MBNL1, PTBP1, hnRNPF, and hnRNPQ-regulated splicing of *Mapt* exon 4. All RT-PCR determinations were made relative to GAPDH or actin (relative expression) and were performed in triplicate. P-value were calculated using one-way ANOVA and mean ± S.D is shown. *p < 0.05; **p < 0.01; ***p < 0.001; ****p < 0.0001.

(C) FMRP-dependent MBNL1, PTBP1, hnRNPF, and hnRNPQ-regulated splicing of *App* exon 8. All RT-PCR determinations were made relative to GAPDH or actin (relative expression) and were performed in triplicate. P-value were calculated using one-way ANOVA and mean ± S.D is shown. *p < 0.05; **p < 0.01; ***p < 0.001; ****p < 0.0001.

(D) FMRP-dependent MBNL1, PTBP1, hnRNPF, and hnRNPQ-regulated splicing of *Tnik* exon 21. All RT-qPCR determinations were made relative to GAPDH or actin (relative expression) and were performed in triplicate. P-value were calculated using one-way ANOVA and mean ± S.D is shown. *p < 0.05; **p < 0.01; ***p < 0.001; ****p < 0.0001.

(E) Summary of exon inclusion/skipping following *Fmr1* and/or splicing factor depletion from N2A cells.

We next examined *App* exon 8, which is also flanked by MBNL1, PTBP1, hnRNPF, and hnRNPQ binding sites, is skipped more frequently upon *Fmr1* depletion compared to control. *Mbnl1* depletion caused *App* exon 8 skipping at the same frequency as *Fmr1* depletion. A double depletion of *Mbnl1* and *Fmr1* was not additive for exon 8 skipping (**Figure 3C**). Depletion of *hnRNPF*, however, caused increased skipping of *App* exon 8 similar to that observed when *Fmr1* was depleted. A double depletion was not additive for exon skipping. *hnRNPQ* depletion did not result in any change in *App* exon 8 skipping. Depletion of these factors had little effect on skipping/inclusion of constitutive *App* exon 2 (**Figure 3- figure supplement 1Q-T**).

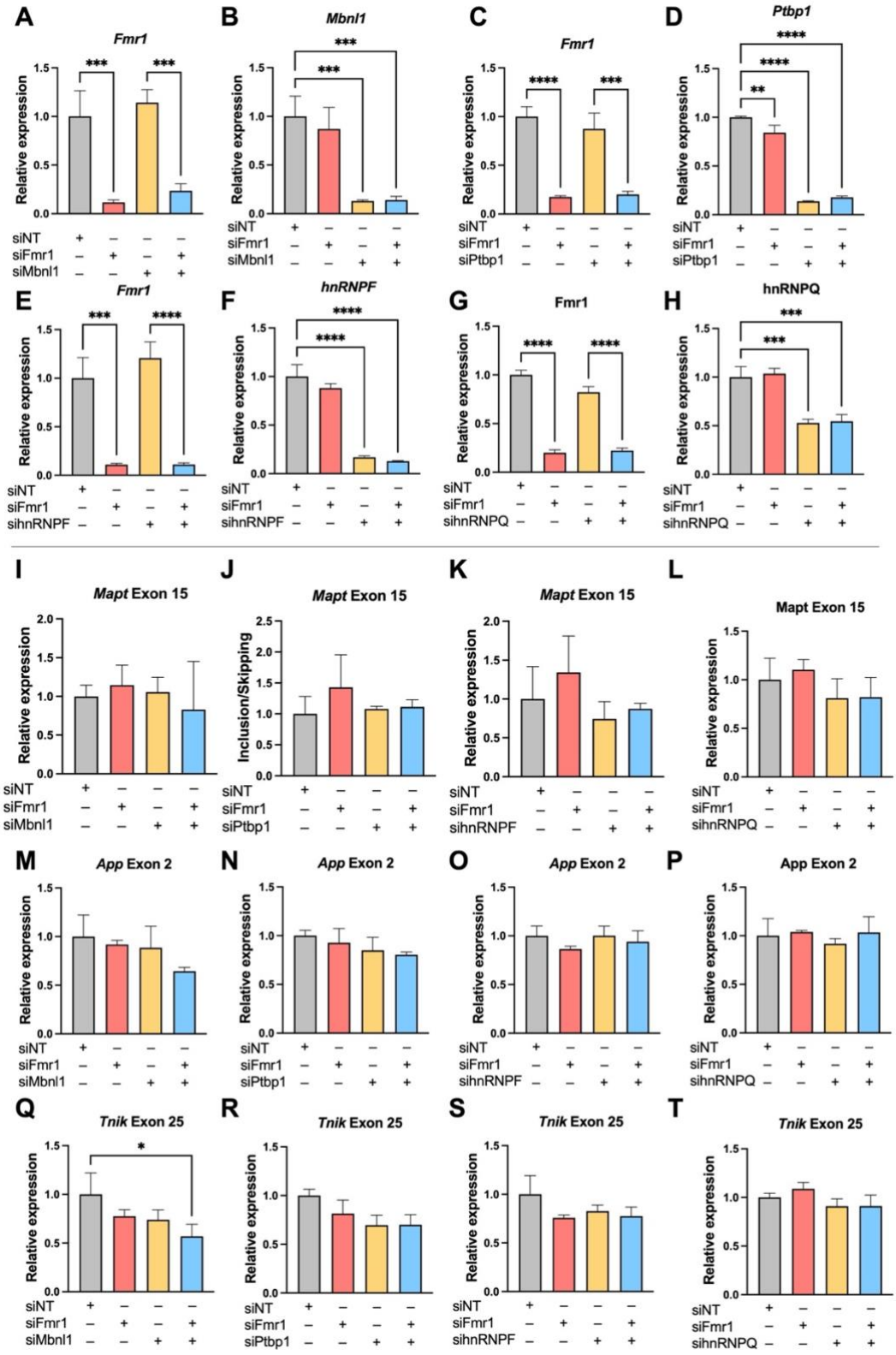

Figure 3 – figure supplement 1. Efficacy of splicing factor depletion and determination of skipping of control exons.

(A-H) Efficacy of *Fmr1* and splicing factor depletion by siRNAs. *p < 0.05; **p < 0.01; ***p < 0.001; ****p < 0.0001 (n=3).

(I-T) Determination of skipping of constitutive exons *Mapt* exon 15, *App* exon 2, and *Tnik* exon 25 following *Fmr1* and splicing factor depletion. *p < 0.05; **p < 0.01 (n=3).

Finally, we examined *Tnik* exon 21, which is flanked by the same splicing factor binding sites, was included more frequently when *Fmr1* is depleted (**Figure 3D**). While *Mbnl1* depletion had no effect on *Tnik* exon 21 skipping/inclusion, depletion of both *Ptbp1* and *hnRNPF* caused greater inclusion relative to controls (**Figure 3D).** Depletion of these factors had little effect on *Tnik* constitutive exon 25 (**Figure 3- figure supplement 1Q-T**). A summary of all these data demonstrates that FMRP regulation of certain splicing factors influences inclusion or skipping of specific exons (**Figure 3E**).

FMRP regulates *Mbnl1* RNA translation and self-splicing

To determine whether FMRP might regulate splicing factor expression directly, we first performed RNA co-immunoprecipitation experiments followed by RT-PCR for splicing factor RNAs. **Figure 4A** demonstrates that FMRP co-immunoprecipitated *Mbnl1* and *Ptbp1* RNAs relative to an IgG control. For comparison, Maurin et al (2018) demonstrated that mouse brain FMRP UV-CLIPs to *Mbnl1* RNA. For comparison, Maurin et al (2018) demonstrated that mouse brain FMRP UV-CLIPs to *Mbnl1* RNA. We further found that around 50% of skipped or included exons in N2A cells contain binding sites for MBNL1 (**Supplementary file 9**) using RBPmap (Paz et al 2014).

Western blotting of the splicing factors showed that MBNL1 and hnRNPQ were elevated ~1.5-2 fold upon *Fmr1*-depletion (**Figure 4B**). Because neither *Mbnl1* nor *hnRNPQ* RNAs are altered by *Fmr1* depletion (**Figure 3- figure supplement 1B and 1H**), we infer that these two RNAs are under negative translational control by FMRP. Furthermore, MBNL1 and hnRNPQ each display

two isoforms; in the case of MBNL1, the slow migrating isoform is reduced when *Fmr1* is depleted while the fast migrating form is increased (**Figure 4B**)**.** For hnRNPQ, the slow migrating isoform is unaffected while the fast migrating isoform is increased upon *Fmr1* depletion (**Figure 4B**). Neither PTBP1 nor hnRNPF undergo abundance changes in *Fmr1*-depleted cells (**Figure 4B and Figure 4- figure supplement 1D and 1F**).

Two of the most frequently alternatively spliced exons of *Mbnl1* mRNA are exon 5 and exon 7 (**Figure 4C**), of which exon5 skipping arises by autoregulated splicing (Terenzi and Ladd 2010; Gates et al 2011; Tran et al 2011) .To determine whether alternative *Mbnl1* auto-splicing is under FMRP control and involves either of these two exons, we performed RT-PCR with primers that distinguish between these exons. **Figure 4D** shows that exon 5 is skipped more frequently upon *Fmr1* depletion while exon 7 and exon 10 (constitutive exon) skipping is unaffected.

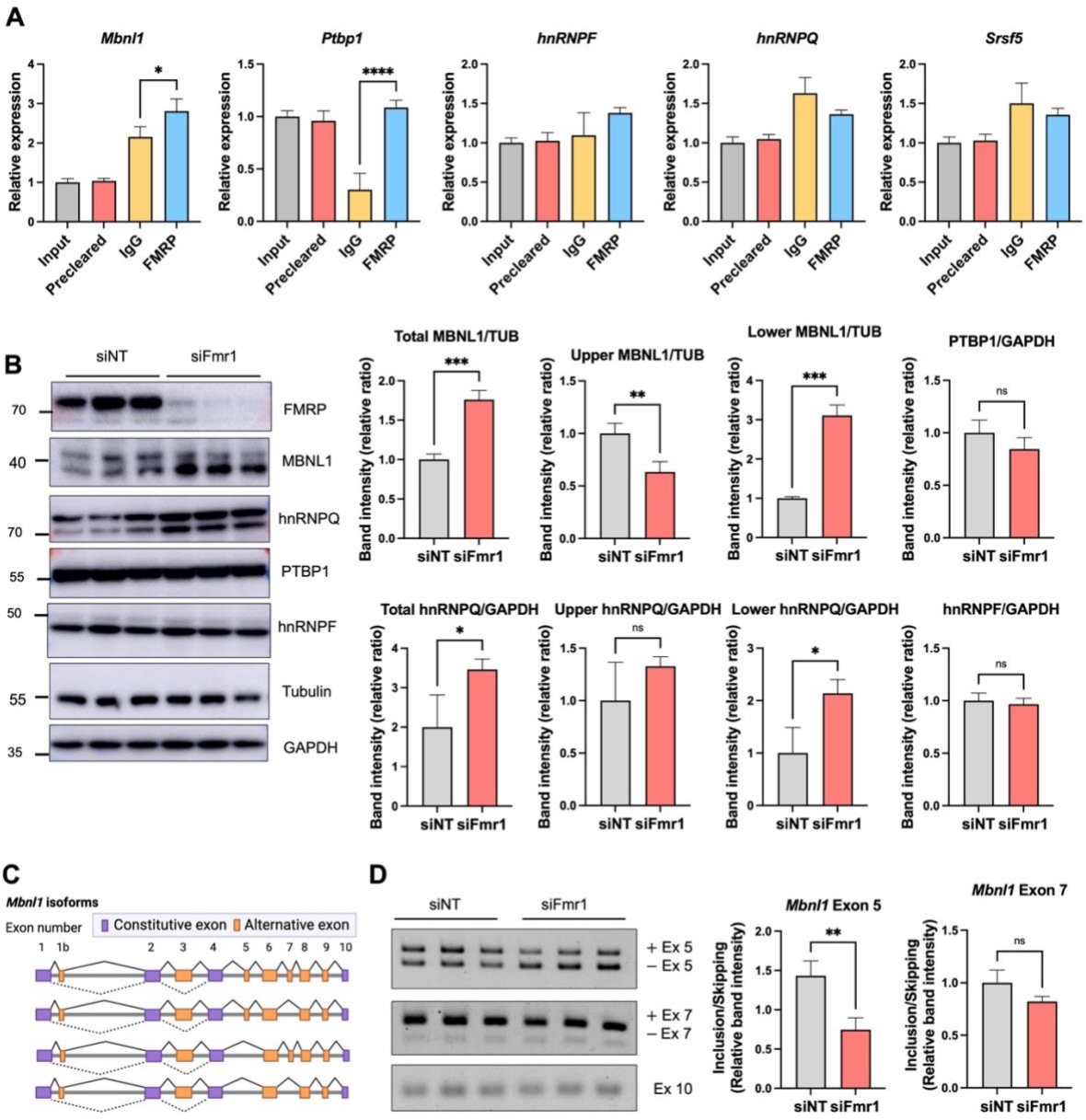

Figure 4. FMRP regulation of *Mbnl1* RNA translation and isoform switching.

(A) Co-immunoprecipitation of *Mbnl1*, *Ptbp1*, *hnRNPF*, *hnRNPQ*, and *Srsf5* RNAs with FMRP. IgG and *Srsf5* RNA served as a immunoprecipitation controls. All experiments were performed in triplicate. P-value were calculated using one-way ANOVA and mean ± S.D is shown. *p < 0.05; ****p < 0.0001.

(B) Western blotting and quantification of splicing factors from control and *Fmr1*-depleted cells. Histogram represents band intensity quantification and mean ± S.D is shown (Student's t-test, *p < 0.05, **p < 0.01, ***p < 0.0001).

(C) Schematic of *Mbnl1* isoforms. Exons 5 and 7 are the most frequently alternatively spliced exons. Created with Biorender.com.

(D) RT-PCR of *Mbnl1* isoforms from control and *Fmr1*-depleted cell. At right is quantification of band intensities of exons 5 and 7 and mean ± S.D is shown (Student's t-test, **p < 0.01). The constitutive exon 10 was amplified to compare total *Mbnl1* RNA expression between the genotypes.

Exon 5, which contains a nuclear localization signal (NLS), determines whether MBNL1 is predominantly nuclear or is distributed to both nucleus and cytoplasm (Tran et al 2011; Kino et al 2015). To assess whether exon 5 skipping upon *Fmr1* depletion alters the nucleus/cytoplasmic ratio of MBNL1, we first performed western blots of protein from cells fractionated into these two compartments. **Figure 5A** shows that MBNL1 containing the NLS encoded by exon 5 (i.e., the upper band) decreased in the cytoplasm following *Fmr1* depletion. Conversely, the NLS-lacking MBNL1 (lower band) increased in the cytoplasm when *Fmr1* was depleted. The upper NLS-containing band was decreased in the nucleus after *Fmr1* depletion. Immunocytochemical analysis of intact cells also shows that the MBNL1 nucleus/cytoplasmic ratio decreased upon *Fmr1* depletion (**FIgure 5B**), which is in concordance with the cell fractionation results.

FMRP shuttles to the nucleus (Tamanini et al 1999) where it has been reported to co-localize with Cajal bodies (Dury et al 2013), membrane-less structures that frequently coincide with the nucleolus. We detected a low amount of FMRP in the nucleus of N2A cells, and considered that it may also associate with splicing factor-rich nuclear speckles (Spector and Lamond 2011). Immunostaining for splicing factor SC35, which detects a few splicing proteins (Ilik et al 2020),

364 showed abundant nuclear speckles but were not co-localized with FMRP, suggesting that FMRP
365 is unlikely to regulate splicing directly (**Figure 5C**).
366
367 Because we had identified a correlation between elevated SETD2, dys-regulated H3K36me3
368 chromatin marks, and altered splicing in *Fmr1* KO mouse hippocampus (Shah et al 2020), we
369 considered this might also occur in FMRP-deficient N2A cells. However, we observed no change
370 in SETD2 levels in these cells, indicating that a changed chromatin landscape and altered splicing
371 in FMRP-deficient cells may not be linked (**Figure 5- figure supplement 1A**).
372

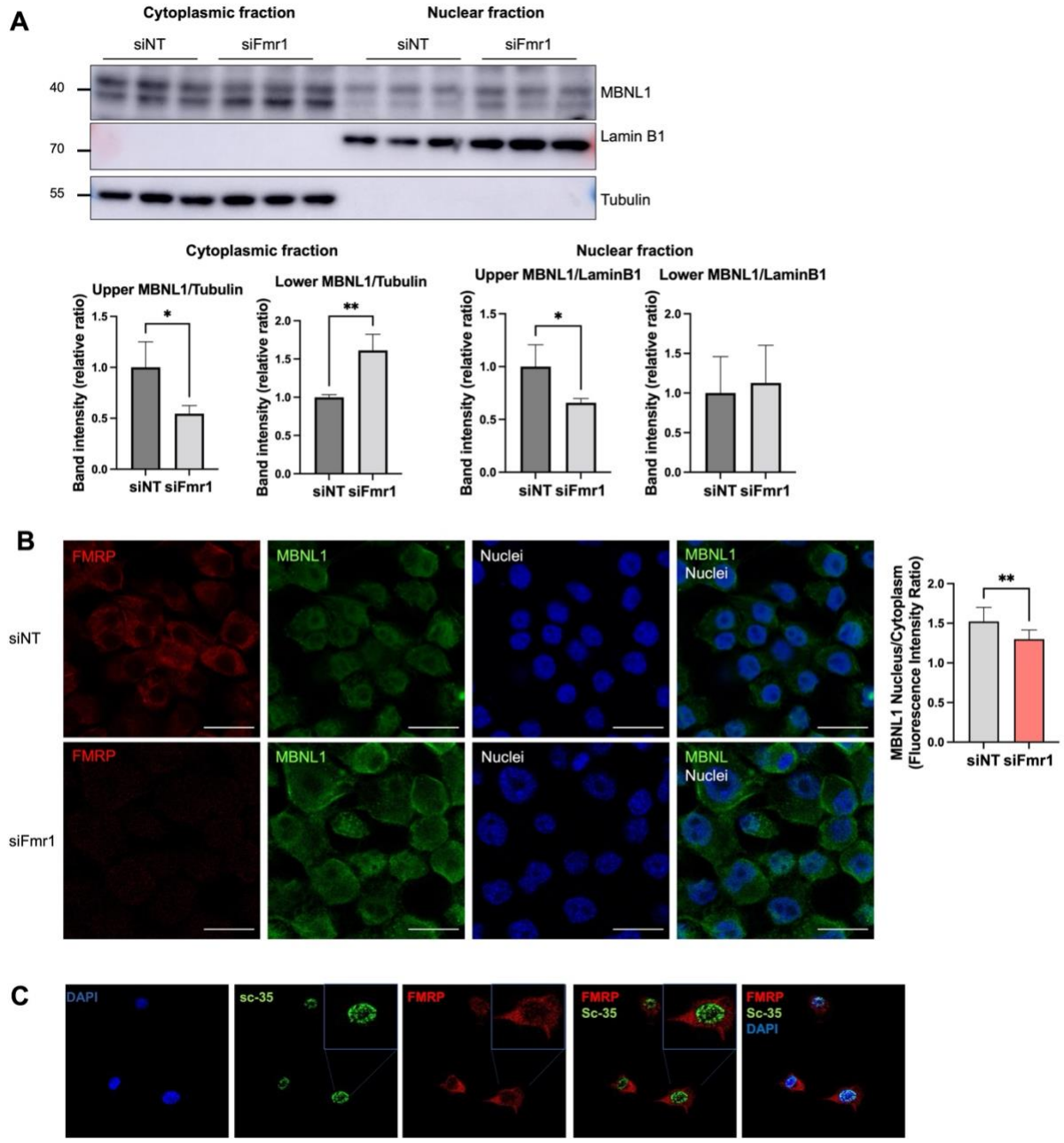

Figure 5. FMRP control of isoform switching regulates nucleus/cytoplasmic distribution of MBNL1.

(A) MBNL1 isoforms in the cytoplasm and nucleus in control and *Fmr1* knockdown cells. Lamin B1 and tubulin served as makers for the nuclear and cytoplasmic fractions, respectively. Quantification of the upper and lower MBNL1 bands relative to tubulin or Lamin B1 is indicated. Mean ± S.D is shown (Student's t-test, *$p < 0.05$, **$p < 0.01$).

(B) Immunocytochemical localization of FMRP, and MBNL1 in N2A cells following *Fmr1* depletion. Quantification of the nucleus/cytoplasmic ratio of MBNL1 fluorescence intensity is at right. Mean ± S.E.M is shown (Student's t-test, **p < 0.01). Magnification 63X. Scale bar, 20 microns.

(C) Immunocytochemistry of FMRP and SC35 in N2A cells. Magnification 63X.

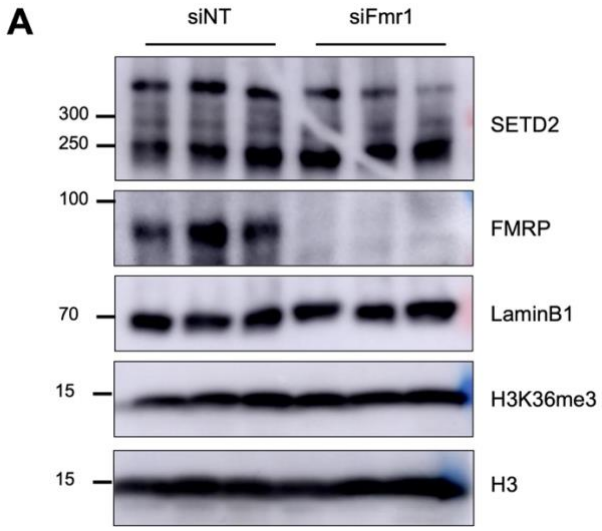

Figure 5 – figure supplement 1. Western blot for SETD2 and H3K36me3 in control and fmr1 depleted N2A cells.

(A) Westerm blot for SETD2, H3K36me3, H3, and FMRP in nuclear extracts of control and *Fmr1* deficient N2A cells. LaminB1 is used as a loading control.

We analyzed published datasets to determine whether *Mbnl1* exon skipping occurs in the FMRP-deficient tissues. **Table 1** shows that exon 5 skipping is detected not only in *Fmr1*-depleted N2A cells, but also in mouse *Fmr1* KO peripheral tissues (liver, muscle, testis). Moreover, exon 7, which is important for MBNL1 self-dimerization, is skipped in several peripheral tissues as well as cerebellum. Although the precise function of the dimerization is unclear, exon 7 residues are thought to increase MBNL1 affinity for RNA (Konieczny et al 2018). Somewhat surprisingly, we did not detect exon 5 skipping in mouse brain, although it and exon 4 were mutually exclusive

exons in human Fragile X postmortem brain. These data show that FMRP-regulated alternative splicing of *Mbnl1* is widespread, but that the exons involved in the splicing events vary according to tissue.

Table 1. Alternative splicing of *Mbnl1* RNA in FMRP-deficient cells and tissues.

Exon number	Domain, function	Species	Sample	Category	Inclusion difference	p. value	Reference
Exon 1	ZnF domain that important for RNA binding and splicing activity [1]	Mouse	LV	SE	-0.146	0.01	This study
Exon 4/Exon 5	ZnF domain that important for RNA binding and splicing activity/NLS [1,2]	Human	Post-mortem cortex	MXE	0.21	0.01	Tran et al., 2019
Exon 5	NLS [1,2]	Mouse	LV	SE	-0.3	0.04	This study
Exon 5	NLS [1,2]	Mouse	MU	SE	0.174	0.0005	This study
Exon 5	NLS [1,2]	Mouse	TE	SE	0.191	0.04	This study
Exon 5	NLS [1,2]	Mouse	N2A	SE	-0.242	0.06	This study
Exon 6	Splicing regulatory domain, encode for bipartite NLS [1]	Mouse	Adult NSC	SE	0.33	0.001	Liu et al., 2018
Exon 6	Splicing regulatory domain, encode for bipartite NLS [1]	Mouse	LV	A3SS	-0.082	0.005	This study
Exon 7	Enhances MBNL1 self-dimerization [2,3]	Mouse	CB	SE	0.093	0.03	This study
Exon 7	Enhances MBNL1 self-dimerization [2,3]	Mouse	MU	SE	0.044	0.03	This study
Exon 7	Enhances MBNL1 self-dimerization [2,3]	Mouse	TE	SE	-0.332	0.0002	This study
Exon 7/Exon 8	Enhances MBNL1 self-dimerization [2,3]	Mouse	MU	MXE	0.051	0.0008	This study
Exon 8	Unknown	Mouse	MU	SE	-0.101	0.0001	This study

[1] López-Martínez et al 2020

[2] Tran et al 2011

[3] Konieczny et al 2014

Figure 6 presents a model depicting FMRP regulation of splicing via MBNL1 in N2A cells. *Mbnl1* pre-mRNA undergoes alternative splicing such that exon 5-containing and exon 5-lacking mRNAs are exported to the cytoplasm. FMRP then binds these mRNAs and limits their translation. The MBNL1 protein that retains the NLS-encoding exon 5 is transported to the nucleus where it regulates alternative splicing of other pre-mRNAs. In *Fmr1*-deficient cells, exon 5-lacking *Mbnl1* RNA is elevated in the cytoplasm relative to exon 5-containing RNA. Because there is no FMRP to limit translation in these cells, MBNL1 synthesis is robust, which is particularly the case for those *Mbnl*1 mRNAs that lack exon 5 NLS. As a consequence, there is reduced MBNL1 transported to the nucleus, which has adverse effects on RNA splicing relative to normal cells. Although this model focuses on MBNL1 in N2A cells, it represents only one of several

418 mechanisms by which FMRP controls splicing. Indeed, as shown in **Figure 3** multiple factors
419 regulate mRNA splicing in an FMRP-dependent manner.

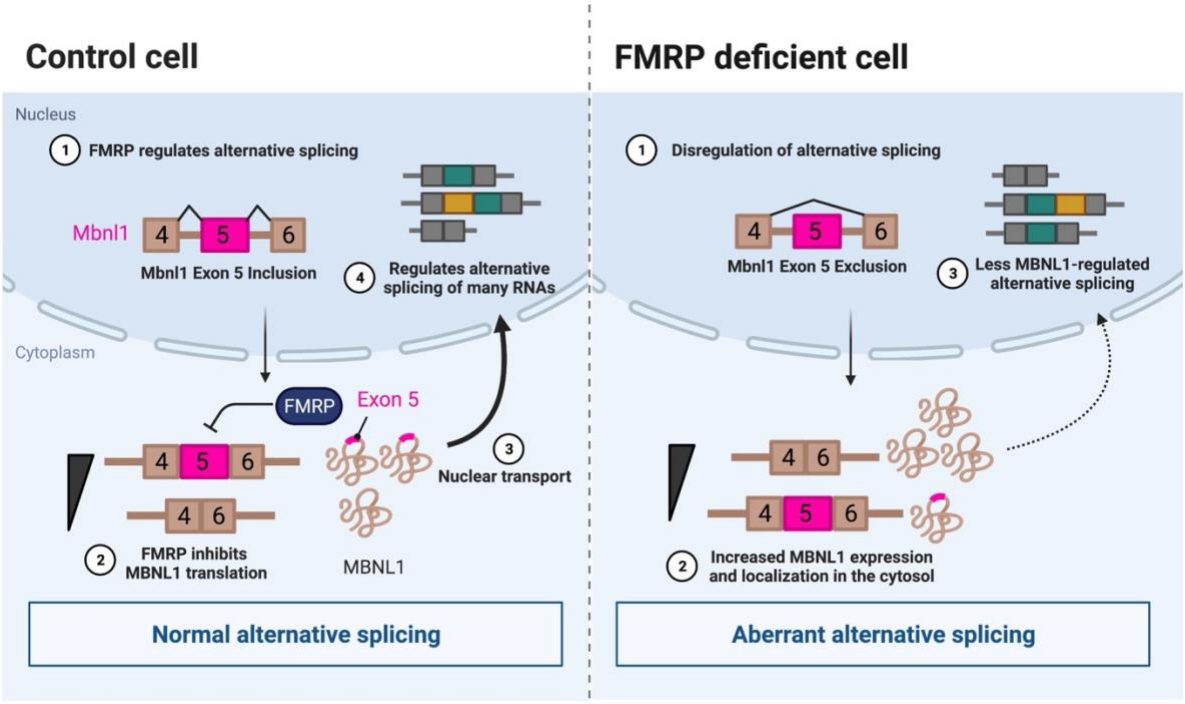

420
421 **Figure 6.** Summary model to explain how FMRP regulates some splicing events through
422 regulation of *Mbnl1* RNA self-splicing and translational control. See text for details. Created with
423 BioRender.com.

Discussion

The proteome of the hippocampus, an exceptionally well-studied brain region of Fragile X Syndrome model mice, is largely attributed to altered mRNA translation with perhaps a minor contribution of protein degradation (Kelleher and Bear, 2008; Huber et al 2015; Bowling et al 2019; Richter and Zhao 2021). This study indicates that mis-regulated alternative splicing almost certainly is a large contributor to the Fragile X proteome not only in the hippocampus and other brain regions of *Fmr1*-deficient mice, but in peripheral tissues as well. Our investigation of the mechanism of FMRP-mediated splicing used *Fmr1*-deficient N2A cells, which was based on the assumption that a single cell type would more likely reveal the involvment of specific factors than a complex mixture of cells such as in the brain. By mapping splicing factor binding sites flanking certain skipped or included exons in 3 mRNAs in *Fmr1*-depleted cells, we found that four proteins: MBNL1, PTB1P, and hnRNPF contribute to alternative splicing mis-regulation. The mRNAs encoding two of these proteins, *Mbnl1* and *hnRNPQ*, are translationally inhibited by FMRP. Moreover, *Mbnl1* self-splicing induced skipping of the NLS-containing exon 5, which is thought to be enhanced by elevated levels of MBNL1 protein (Konieczny et al 2014), was observed. This event impairs MBNL1 nuclear transport, which in turn likely affects downstream splicing decisions. *Mbnl1* exon 5 is also skipped in *Fmr1*-deficient mouse peripheral tissues as well as in human postmortem Fragile X brain. Exons 6, 7, and 8 are skipped in neural stem cells, and/or liver, muscle, testis, and cerebellum from *Fmr1*-deficient mice. Thus, FMRP regulation of *Mbnl1* splicing is complex and is strongly influenced by cell/tissue-type, which likely contributes to downstream splicing regulation.

The regulation of splicing via MBNL1 is only one of several FMRP-dependent mechanisms that mediate RNA processing. PTBP1, hnRNPF, and hnRNPQ all influence splicing decisions that are downstream of FMRP. For both MBNL1 and hnRNPQ, this involves FMRP-regulated translation

of their respective mRNAs. In this sense, FMRP control of splicing is similar to FMRP control of chromatin modifications and transcription; the root cause of the alteration of these molecular events is dys-regulated translation when FMRP is absent (Korb et al 2017; Shah et al 2020). We also considered whether FMRP might influence splicing directly. It is a nuclear shuttling protein that at least in mouse testis, binds chromatin and is involved in the DNA damage response (Alpatov et al 2014). FMRP co-localizes with Cajal bodies in Hela cells, which implies it may modify rRNA biogenesis (Dury et al 2013). We inferred that if FMRP was a direct regulator of splicing, it would co-localize with SC35-containing nuclear splicing/processing bodies or speckles (Spector and Lamond 2011). We did not detect any such co-localization and thus FMRP is unlikely to be a direct modulator of splicing. In addition, we previously reported a correlation between the up-regulation of SETD2, altered H3K36me3 chromatin marks, and RNA splicing mis-regulation in *Fmr1*-deficient mouse brain (Shah et al 2020). In *Fmr1* KO N2A cells, however, we detected no alteration in SETD2 levels, and thus a change in H3K36me3 leading to splicing dys-regulation is unlikely.

In most cases, the dys-regulated inclusion/exclusion of exons in *Fmr1*-deficient tissues/cells has a mean of ~20%, but with a large distribution. Although the magnitude of such changes is within the range often observed for alternative splicing (Tapial et al 2017), it is unclear to what extent these splicing changes have biological consequnces. However, even modest changes in exon skipping can manifest themselves with changes in biology if a skipped exon is regulatory. For example, an exon encoding a regulatory phosphorylation site in the RNA binding protein CPEB4 is skipped <30% of the time but this skipping is correlated with if not causative for autism (Parras et al 2018). In the *Fmr1* KO mouse, we cannot ascribe any single mis-splicing event as contributing to a Fragile X phenotype. Instead, it is more likely that the amalgamation of hundreds of mis-splicing events result in some Fragile X pathophysiology, for example, dys-regulated synaptic transmission or learning and memory (Huber et al 2000; Udagawa et al 2013).

Finally, the dys-regulated splicing in Fragile X model mice may represent a point of convergence with other neurodevelopmental disorders (Shah and Richter 2021). For example, splicing is impaired in autism spectrum disorders (Irimia et al 2014), Rett Syndrome (Li et al 2016), Pten (Thacker et al 2020), and others (Shah et al 2021). Whether mis-splicing in these disorders are related mechanistically is unclear, but they may involve several of the same factors (e.g., MBNL1, PTBP1). More intriguing is the prospect that some mis-splicing events link similar behavioral or other physiological impairments among these disorders. This may especially be the case when very small microexons encoding regulatory domains are skipped (Gonatopoulos-Pournatzis and Blencowe 2020). Future studies will be necessary determine whether specific mis-splicing events promote pathophysiolgical outcomes.

Materials and Methods

Animals

Mice were housed under a 12 h light/dark cycle with free access to food and water. Wild-type and *Fmr1* KO mice were purchased from the Jackson Laboratories. Two to three month old male mice were used in this study (n=3 each for WT and *Fmr1* KO). Animal maintenance and experimental procedures were performed accordance with all animal research guidelines from University of Massachusetts Chan Medical School.

Cell culture and siRNA transfection

Mouse N2A cells were cultured in Dulbecco's Modified Eagels Medium (DMEM) supplemented with 10% fetal bovine serum (FBS) and antibiotics. The siRNAs targeting *Fmr1*, *Ptbp1, hnRNPF*, *hnRNPQ,* and *Mbnl1* were purchased from IDT. As a negative control siRNA, siNT (ON-TARGETplus) was purchased from Dharmacon. For siRNA transfection, $1x10^5$ cells were seeded in 6-well plates overnight and transfected with 20-25 pmol of the indicated siRNAs using Lipofectamine 3000 (ThermoFisher Scientific, 13778030) following the manufacturer's instructions. For double depletion experiments, cells were transfected in triplicate as follows: 1) siNT (80 pmol), 2) siFmr1 (40 pmol) + siNT (40 pmol), 3) siMbnl1 (40 pmol) + siNT (40 pmol), 4) siFmr1 (40 pmol) + siMbnl1 (40 pmol). Cells were incubated with the indicated siRNAs for 48-72 h before being analyzed.

RT-PCR and qPCR

Total RNA was isolated using TRIzol-LS (Invitrogen, 10296-028) and total RNA (1 µg) was reverse transcribed using QuantiTect Reverse Transcription Kit (Qiagen, 205313) according to manufacturer's instructions. RT-PCR was performed using GoTaq Green Master Mix (Promega, M7123). 2 µl of diluted cDNA was added to 12.5 µl GoTaq Green Master Mix and 0.4 µM of

forward and reverse primers and nuclease-free water in a 25 µl reaction. PCR amplification was performed as follow: initial denaturation at 95 °C for 2 min, 30 cycles of denaturation at 95 °C for 30 s, annealing at each primer's annealing temperature for 1 min, and 72 °C for 1 min/kb and final extension at 72 °C for 5min. qPCR was performed with QuantStudio3 (ThermoFisher Scientific) as follow: initial denaturation at 95 °C for 10 min, 39 cycles of denaturation at 95 °C for 15 s annealing and extension at 60 °C for 1 min. Exon inclusion and exclusion levels were quantified using qPCR. For alternative splicing validation, primers were designed to specifically amplify exon-exon junctions of the included or skipped isoform. A primer pair amplifying a constitutive exon in each mRNA was used to determine changes in total mRNA expression between genotypes. Primer sequence information is listed below.

Western blot

Cells were washed with ice-cold PBS and collected using trypsin to release them from the plasticware. After centrifugation, the cells were lysed with ice-cold RIPA buffer (NaCl 150 mM, Triton X-100 1%, sodium deoxycholate 0.5%, SDS 0.1% and Tris-HCl 50 mM pH 8.0) with cOmplete Mini EDTA-free protease inhibitor cocktail (Sigma, 11836170001) and PhosSTOP (Sigma, 4906837001) and rotated for 10 min at 4 °C. The lysates were collected by centrifugation at 12,000 rpm for 10 min at 4 °C. Supernatants were removed and the protein concentration was quantified using the colorimetric assay by Pierce™ BCA protein assay kit (ThermoFisher Scientific, 23225). Protein lysates were resolved using 10% SDS-PAGE gels and transferred to 0.45 µm PVDF membranes (Millipore, IPVH00010). The membranes were blocked in 5% skim milk solution for 1 h at RT then incubated with primary antibody at 4 ℃ overnight: Anti-FMRP antibody (Abcam, ab17722, 1:1,000), anti-GAPDH antibody (Cell signaling technology, 2118, 1:1,000), anti-alpha-Tubulin (Sigma, T5168, 1:1,000), anti-Lamin B1(Abcam, ab16048, 1:2,000), anti-MBNL1 (Cell signaling technology, 94633, 1:1,000), anti-PTBP1 (Cell signaling technology,

57246, 1:1,000), anti-hnRNPF (Novusbio, NBP2-57442-25 µl, 1:1,000), anti-hnRNPQ (Abclonal, A9609, 1:1,000), anti-SETD2 (Abclonal, A11271, 1:1,000), anti-histone H3K36me3 (Abcam, ab9050, 1:1000), anti-histone H3 (Abcam, ab18521, 1:1000). The membranes were incubated with horse radish peroxidase (HRP)-linked secondary anti-rabbit (Jackson ImmunoResearch, 211-032-171, 1:5,000) or anti-mouse (Jackson ImmunoResearch, 115-035-174, 1:5,000) antibody and developed with ECL (Pierce, NEL105001EA). Immunoreactive bands were detected using GE Amersham Imager.

Cytosol and nuclear protein fractionation

Cells were washed with ice-cold PBS, collected by trypsinization, pellets collected by centrifugaiotn, and then resuspended in Triton extraction buffer (TEB, PBS containing 0.5% triton X-100 (v/v), 2 mM phenylmethylsulfonyl fluoride, 0.02% NaN_3) and lysed on ice for 10 min. Following a centrifugation at 12,000 rpm at 4 °C, the supernatants were saved for cytoplasmic protein and the pellets were resuspended in nuclear lysis buffer (50 mM Tris-HCl pH 7.4, 120 mM NaCl, 1 mM EDTA, 1% Triton X-100, 0.1% SDS) and lysed by sonication at high power for 8 cycles (15 sec on, 60 sec off) using a Bioruptor (Diagenode). The lysates were collected after centrifugation at 13,000 rpm for 10 min at 4 °C and the supernatants were prepared for nuclear protein analysis. Nuclear and cytoplasmic protein concentrations were measured using BCA assays.

RNA-seq

Mouse tissues were powdered in liquid nitrogen with a frozen mortar and pestle. For RNA extraction, TRIzol was added to the tissue powder and homogenized with Dounce tissue homogenizer. The RNA was treated with TurboDNase (Invitrogen, AM2238) to remove genomic DNA contamination. For peripheral tissues and N2A cells, total RNA was extracted and the

565 integrity analyzed by a fragment analyzer. Library preparation and RNA sequencing were
566 performed by Novogene (CA, USA). For brain samples, polyadenylated mRNA was enriched
567 using Nextflex Poly(A) Beads (NEXTflex, Bioo Scientific Corp, 512980) and cDNA libraries were
568 prepared using a NEXTflex Rapid Directional qRNA-Seq Kit (Bioo Scientific Corp, NOVA-5130-
569 03D). In brief, the mRNA was randomly fragmented, reverse transcribed, and double-stranded
570 cDNA was adenylated and ligated to index adapters. The cDNA was amplified by PCR and
571 purified with AMPure beads (Beckman Coulter, A63881). The libraries were quantified with a
572 KAPA Library Quantification Kit (KAPA Biosystems, KK4873) and the quality and size were
573 analyzed by a fragment analyzer. Pooled libraries were sequenced on an NextSeq500 Sequencer
574 using NextSeq 500/550 High Output Kit v2.5 (Illumina, 20024906, 75 base paired ends).
575
576 **Differential expression and alternative splicing analysis**
577 RNA-seq analysis was performed using DolphinNext pipeline at UMass Chan Medical School
578 (Yukselen et al 2020). Quality trimming was conducted using Fastqc (v0.11.8) and Trimmomatic
579 (v.0.39). Reads below a minimum quality PHRED score of 15 at the 10nt sliding window were first
580 clipped and the clipped reads shorter than 25nt were trimmed. The trimmed reads were mapped
581 to rRNA by Bowtie2 (v2.3.5) were further filtered out. The cleaned reads were aligned to the
582 mouse reference genome (mm10) with STAR (v1.16.1), and gene expression was quantified by
583 RSEM (v1.3.1). Differential gene expression was analyzed using DESeq2 (v1.16.1). The FDR
584 adjusted p-value < 0.05 and log2FC > 0.2 or < -0.2 was used as the cut-offs to identify the
585 differentially expressed genes. Alternative splicing events are analyzed using rMATS (v3.0.9)
586 (Shen et al 2014) and p-value and PSI > 0.05 was used as the cut-offs for splicing events. To
587 assess biological function, Gene Ontology (GO) term analysis was conducted using clusterProfiler
588 R package (Wu et al 2021, Yu et al 2012). Significant RNA Overlap from WT and *Fmr1* KO
589 hippocampus, cortex, and cerebellum was analyzed using DynaVenn (Amand et al 2019) using
590 p-value ordered RNA list.

Generation of an *Fmr1* CRISPR/Cas9-edited cell line

To construct an *Fmr1* KO N2A mouse cell line, an *Fmr1* exon 3 DNA oligonucleotide was inserted into pLentiCRISPR (Addgene, 49535) adapted from published methods (Li et al 2020). Briefly, annealed and phosphorylated oligonucleotides were cloned into a FastDigest BmsBI (Fermentas)-digested vector following the manufacturer's protocol. pLentiCRISPR-m*Fmr1*Exon3 was co-transfected with pMD2.G and psPAX2 into HEK293T cells. The viral particles containing supernatants were collected after 48 h of transfection by filtering through 0.45 µm filters and transduced to N2A cells. After 3 days of infection, transduced cells were selected with puromycin for 2 weeks. Puromycin resistant cells were seeded in each well of a 96 well plate with a single cell per well. Single cell-derived colonies were obtained after several weeks of culture and verified for *Fmr1* knockout by Sanger DNA sequencing and western blotting. For the sequencing, genomic DNA was extracted using lysis buffer (10 mM Tris 8.0, 200 mM NaCl, 20 mM EDTA. 0.2% Triton X-100 and 100 µg/ml proteinase K) and the deleted exon region was PCR amplified using primers (sequences noted below). To identify deleted sequences, the PCR products were cloned with a TOPO TA Cloning Kit (ThermoFisher Scientific, 450030) followed by sequencing using T7 primers (Genewiz).

Alternative splicing reporter system

To generate an alternative splicing reporter, total DNA was isolated from N2A cells using the lysis buffer described above. *Mapt* exon 4 and flanking the intron regions were PCR amplified using Phusion High-Fidelity DNA polymerase and inserted into NheI/BamHI digested pFlareA Plasmid (Addgene, 90249) and sequenced. Cultured N2A control and *Fmr1* CRISPR/Cas9 KO cells were seeded in 6-well plates overnight and then transfected using 7.5 µl of Lipofectamine 3000 (Invitrogen) and 5 µl of P3000 with the 1 µg of pFlareA-Mapt exon4 splicing reporter. For the rescue experiment, 1.5 µg of pcDNA-myc or pcDNA-mouse FMRP ectopic expression plasmids

was added. Transfected cells were washed with PBS and collected by trypsinization 48 h after transfection. GFP and mCherry fluorescence intensities were detected using flow cytometry (LSR II A-5 Donald).

RNA-Immunoprecipitation (RNA-IP)

N2A cells were transfected with siNT and siFmr1 using Lipofectamine 3000. After 72 h of incubation, the cells were washed with fresh media containing 100 µg/ml cycloheximide (CHX, Sigma, C4859). After washing with ice-cold PBS-containing CHX, the cells were pelleted and lysed in 1X polysome buffer [20 mM Tris-HCl pH 7.5, 5 mM $MgCl_2$, 100 mM KCl, 1 mM DTT, 100 µg/ml CHX, protease inhibitor cocktails, 1 % Triton X-100 (v/v)] with 10 passages through a 25 G needle to triturate and incubated on ice for 10 min. The lysates were centrifuged at 14,000 x *g* at 4 °C and RNA concentration was measured using Qubit BR RNA Assay Kits (ThermoFisher Scientific, Q10210). For IP, 5 µg of RNA was precleared with 25 µl of Protein G Dynabeads (Invitrogen, 10003D) for 30 min at 4 °C. 10% of aliquot of the precleared lysates were saved as an input. 2.5 µg of FMRP antibody (Abcam, ab17722) or IgG (Sigma, 12-370) was added to the precleared lysates and incubated for 2 h at 4 °C. 25 µl of Protein G Dynabeads was added and incubated for 30 min at 4 °C and the beads were gently washed with wash buffer [20 mM Tris-HCl, 100 mM KCl, 5 mM $MgCl_2$, 1% Triton X-100 (v/v)] for 3 times. RNA was extracted using TRIzol and 100 ng of RNA were reverse transcribed using Quantitect followed by qPCR using iTaq SYBRgreen (Bio-rad, 1725122).

Immunocytochemistry

For immunofluorescent staining, $1x10^5$ cells were seeded in a Chamber Slide (Nunc Lab-Tek II CC2, 154917) and transfected with 10 pmol siNT and siFmr1. After 48 h, cells were washed and fixed with 4 % formaldehyde solution (ThermoFisher Scientific, AAJ19943K2) for 10 min at RT.

The fixed cells were washed with PBS three times and permeabilized using 0.1% Triton X-100 in PBS for 15 min at RT. The cells were washed with PBS three times and incubated with blocking buffer (1% BSA in PBS) for 1h at RT. Cells were then incubated overnight at 4 °C with primary antibodies anti-FMRP (Abcam, Ab17722, 1:500), anti-MBNL1 (TheromoFisher, 66837-IG, 1:100) or anti-Sc35 (Millipore Sigma, S4045, 1:1000) and incubated with the secondary antibodies using Alexa 488-labeled goat anti-mouse IgG (Abcam, Ab150113, 1:1000), Alexa 594-labeled goat anti-rabbit IgG (ThermoFisher, A-10012, 1:250). Hoechst 33342 was used to stain the cell nuclei at 0.2 µg/ml for 15 min. Coverslips were mounted using FlourSave reagent (Milipore, 345789). Images were acquired using a Zeiss confocal microscope LSM900.

Data availability

RNA-seq datasets are available in GEO (accession number GSE207145).

Primers for validation of altenative splicing

Dcun1d2 Ex5 F	ATGGCTGTTGCATATTGGAAGTT
Dcun1d2 Ex7 R	CAGGCGGCTTCTAAAGCACT
Dcun1d2 Ex2 F	GCTCAGAAGGACAAGGTCCG
Dcun1d2 Ex2 R	TAGACTCTCGGTGAAACGCC
Tnik SJC F	CGGCCAGCTGATCTGACG
Tnik SJC R	CTCACTGCTCTCCGACTCCT
Tnik IJC F	AAGTCCGAAGGATCACCCGT
Tnik IJC R	TGCCGTCAGATCCTCATCTAT
Tnik Ex20 F	ATCCAGAGACATCACACGGC
Tnik Ex22 R	TTCAGGGGGCGGTTTGTTT
Tnik Ex25 F	GGCCAAACTCAATGAAGCGA
Tnik Ex25 R	GGTGTGTCACTATGAGGGCG
Ski IJC F	GTGCCCCGGGTCTCA
Ski IJC R	GACGTCTCTTTCTCACTCGC
Ski SJC F	CCTGCCACTGGGGCTTC
Ski SJC R	AGCCGAGGCTCCGGG

Wnk1 SJC F	CAGGGAATACAGCCAACTGTTC
Wnk1 SJC R	ACTCCCTGAGTACTCTGTGTTC
Wnk1 IJC F	ACCTTGGCTTCATCTGCTACA
Wnk1 IJC R	TGAGTACTCTGGTACAAAACATCT
App SJC F	TGCTCTGAACAAGCCGAGAC
App SJC R	CTGTCGTGGGAAACACGCTG
App IJC F	GCAGCGTGTCAACCCAAAG
App IJC R	GGGACATTCTCTCTCGGTGC
Mapt SJC F	TGAACCAGTATGGCTGACCC
Mapt SJC R	GCTGGCCACACGAGCTTTTA
Mapt IJC F	TGGCTTAAAAGCCGAAGAAGC
Mapt IJC R	TCTTCTCGTCATTTCCTGTCCTG
Os9 SJC F	TGGACAAACTCATCAAGAGGCT
Os9 SJC R	AATCTTGCCTGTAGGGTGTGG
Os9 IJC F	ACCCTACAGAGGAGGAACCTG
Os9 IJC R	CAATCTTGCCTTCCGCCGTG
Mapt Ex15 F	AAAATCCGGAGAACGAAGCG
Mapt Ex15 R	AGGCGGCTCTTACTAGCTGA
App Ex2 F	TCGCCATGTTCTGTGGTAAAC
App Ex2 R	AATGCAGGTTTTGGTCCCTGA
Mbnl1 Ex5 IJC F	AGCTGCCATGACTCAGTCGG
Mbnl1 Ex5 IJC R	GAGGAATTCCCAGGTCAAAGGT
Mbnl1 Ex7 IJC F	CTACTGCAGCTGCCATGGGAAT
Mbnl1 Ex7 IJC R	AAGAGCAGGCCTCTTTGGCAAT
Mbnl1 Ex10 F	ATGGTGAGGGAGGGAACTGA
Mbnl1 Ex10 R	GGTACTTAAAGCCATGGTGTGC
Mbnl1 Ex5 IJC F	AGCTGCCATGACTCAGTCGG
Mbnl1 Ex5 IJC R	GAGGAATTCCCAGGTCAAAGGT
Mbnl1 Ex5 SJC F	CTACTGCAGCTGCCATGGGAAT
Mbnl1 Ex5 SJC R	AAGAGCAGGCCTCTTTGGCAAT

655

Primers for pFlareA reporter cloning

NheI-Mapt Ex4-BamHI-F	GCTAGCTAGCTTCTGGGTACA
NheI-Mapt Ex4-BamHI-R	CGCGGATCCAAGCGTATCTGTGAC

656

Primers for qPCR

Mbnl1 F	AGCTGTACTTCCCCCATTGC
Mbnl1 R	AGCGGGTGTCATGCACAATA
Ptbp1 F	AGTGCGCATTACACTGTCCA
Ptbp1 R	CTTGAGGTCGTCCTCTGACA
hnRNPF F	CCACTCAACCCTGTGAGAGT
hnRNPF R	TTGCTAGCCCCTGTTGTTGA
hnRNPQ F	AGCCCATGGATACTACTTCAGC
hnRNPQ R	ATGTGCAACTAGCCCTGCAA
Srsf5 F	GGTGACGATTGAACATGCCC
Srsf5 R	CGACTGCTAAAACGGTCGGA

657

658

Primers for construction of CRISPR/Cas9 KO cell line

mFmr1-sgE3-F	CACCGTATTATAACCTACAGGTGGT	sgRNA for pLenticrispr
mFmr1-sgE3-R	AAACACCACCTGTAGGTTATAATAC	sgRNA for pLenticrispr
mFmr1 E3 GT F	ACCAAGAAAGAGTCACATTTAACCA	Deletion genotype primer
mFmr1 E3 GT R	GGGGTAAAGAAACTTGGGACA	Deletion genotype primer

659

660

Acknowledgments

We thank Ms. SitharaRaju Ponny for advice on bioinformatic and statistical analysis and Dr. Heleen van't Spijker for assistance with immunofluorescence microscopy. We thank Dr. Mariya Ivshina for insightful conversations related to this study and Drs. Pablo Visconti and Maria Gracia Gervasi (University of Massachusetts Amherst) for assistance with some initial experiments. This work was supported by NIH grants GM046779, GM135087, UL1-TR001453, and a grant from FRAXA. SS was a FRAXA postdoctoral fellow.

Competing interests

All authors declare no financial or non-financial competing interests.

References

Akerman A, David-Eden H, Pinter RY, Mandel-Gutfreund Y (2009**). A computational approach for genome-wide mapping of splicing factor binding sites.** *Genome Biology* **10**:R30. https://doi.org/10.1186/gb-2009-10-3-r30

Alpatov R, Lesch BJ, Nakamoto-Kinoshita M, Blanco A, Chen S, Stützer A, Armache KJ, Simon MD, Xu C, Ali M, Murn J, Prisic S, Kutateladze TG, Vakoc CR, Min J, Kingston RE, Fischle W, Warren ST, Page DC, Shi Y (2014). **A chromatin-dependent role of the fragile X mental retardation protein FMRP in the DNA damage response.** *Cell* **157**:869-881. https://doi.org/10.1016/j.cell.2014.03.040

Amand, J., Fehlmann, T., Backes, C., & Keller, A. (2019). **DynaVenn: web-based computation of the most significant overlap between ordered sets.** BMC bioinformatics, **20**: 1-5. https://doi.org/10.1186/s12859-019-3320-5

Bhattacharya S, Levy MJ, Zhang N, Li H, Florens L, Washburn MP, Workman JL (2021). **The methyltransferase SETD2 couples transcription and splicing by engaging mRNA processing factors through its SHI domain.** *Nature Communications* **12**:1443. https://doi.org/10.1038/s41467-021-21663-w

Bowling H, Bhattacharya A, Zhang G, Alam D, Lebowitz JZ, Bohm-Levine N, Lin D, Singha P, Mamcarz M, Puckett R, Zhou L, Aryal S, Sharp K, Kirshenbaum K, Berry-Kravis E, Neubert TA, Klann E (2019). **Altered steady state and activity-dependent de novo protein expression in fragile X syndrome.** *Nature Communications* **10**:1710. https://doi.org/10.1038/s41467-019-09553-8

Darnell JC, Van Driesche SJ, Zhang C, Hung KY, Mele A, Fraser CE, Stone EF, Chen C, Fak JJ, Chi SW, Licatalosi DD, Richter JD, Darnell RB (2011**). FMRP stalls ribosomal translocation on mRNAs linked to synaptic function and autism.** *Cell* **146**:247-261. https://doi.org/10.1016/j.cell.2011.06.013

Das Sharma S, Metz JB, Li H, Hobson BD, Hornstein N, Sulzer D, Tang G, Sims PA (2019). **Widespread Alterations in Translation Elongation in the Brain of Juvenile Fmr1 Knockout Mice.** *Cell Reports* **26**:3313-3322. https://doi.org/10.1016/j.celrep.2019.02.086

Dölen G, Osterweil E, Rao BS, Smith GB, Auerbach BD, Chattarji S, Bear MF. (2007**) Correction of fragile X syndrome in mice.** *Neuron* **56**:955-962. https://doi.org/10.1016/j.neuron.2007.12.001

Dury AY, El Fatimy R, Tremblay S, Rose TM, Côté J, De Koninck P, Khandjian EW (2013). **Nuclear Fragile X Mental Retardation Protein is localized to Cajal bodies.** *PLoS Genetics* **9**:e1003890. https://doi.org/10.1371/journal.pgen.1003890

El Fatimy R, Davidovic L, Tremblay S, Jaglin X, Dury A, Robert C, De Koninck P, Khandjian EW (2016). **Tracking the Fragile X Mental Retardation Protein in a Highly Ordered Neuronal RiboNucleoParticles Population: A Link between Stalled Polyribosomes and RNA Granules.** *PLoS Genetics* **12:**e1006192 https://doi.org/10.1371/journal.pgen.1006192

Feng Y, Absher D, Eberhart DE, Brown V, Malter HE, Warren ST (1997). **FMRP associates with polyribosomes as an mRNP, and the I304N mutation of severe fragile X syndrome abolishes this association.** *Molecular Cell* **1:**109-118. https://doi.org/10.1016/s1097-2765(00)80012-x

Gates DP, Coonrod LA, Berglund JA (2011) **Autoregulated splicing of muscleblind-like 1 (MBNL1) Pre-mRNA.** *Journal of Biological Chemistry* **286**:34224-4233. https://doi.org/10.1074/jbc.M111.236547

Gonatopoulos-Pournatzis T, Blencowe BJ (2020). **Microexons: at the nexus of nervous system development, behaviour and autism spectrum disorder.** *Current Opinion in Genetcis and Development* **65**:22-33**.** https://doi.org/10.1016/j.gde.2020.03.007

Hagerman RJ, Berry-Kravis E, Hazlett HC, Bailey DB Jr, Moine H, Kooy RF, Tassone F, Gantois I, Sonenberg N, Mandel JL, Hagerman PJ (2017). **Fragile X syndrome.** *Nature Reviews Discovery Primers* **3**:17065. https://doi.org/10.1038/nrdp.2017.65

Hale CR, Sawicka K, Mora K, Fak JJ, Kang JJ, Cutrim P, Cialowicz K, Carroll TS, Darnell RB (2021). **FMRP regulates mRNAs encoding distinct functions in the cell body and dendrites of CA1 pyramidal neurons.** *Elife* **10:**e71892. https://doi.org/10.7554/eLife.71892

Huber KM, Kayser MS, Bear MF (2000). **Role for rapid dendritic protein synthesis in hippocampal mGluR-dependent long-term depression.** *Science* **288**:1254-1257. https://doi.org/10.1126/science.288.5469.1254

Huber KM, Klann E, Costa-Mattioli M, Zukin RS (2015). **Dysregulation of Mammalian Target of Rapamycin Signaling in Mouse Models of Autism.** *Journal of Neuroscience* **35**:13836-13842. https://doi.org/10.1523/JNEUROSCI.2656-15.2015

Ilik İA, Malszycki M, Lübke AK, Schade C, Meierhofer D, Aktaş T (2020). **SON and SRRM2 are essential for nuclear speckle formation.** *Elife* **9**:e60579. https://doi.org/10.7554/eLife.60579

Irimia M, Weatheritt RJ, Ellis JD, Parikshak NN, Gonatopoulos-Pournatzis T, Babor M, et al. (2014). **A highly conserved program of neuronal microexons is regulated in autistic brains**. *Cell* **159**:1511–1523. https://doi.org/10.1016/j.cell.2014.11.035

Kelleher RJ 3rd, Bear NF (2008). **The autistic neuron: troubled translation?** *Cell* **135**:401-406. https://doi.org/10.1016/j.cell.2008.10.017

Kim S, Kim H, Fong N, Erickson B, Bentley DL (2011). **Pre-mRNA splicing is a determinant of histone H3K36 methylation.** *Proceedings of the National Academy of Sciences U S A.* **108:**13564-13569. https://doi.org/10.1073/pnas.1109475108

Kino Y, Washizu C, Kurosawa M, Oma Y, Hattori N, Ishiura S, Nukina N (2015). **Nuclear localization of MBNL1: splicing-mediated autoregulation and repression of repeat-derived aberrant proteins.** *Human Molecular Genetics* **24**:740-56.
https://doi.org/10.1093/hmg/ddu492

Kolasinska-Zwierz P, Down T, Latorre I, Liu T, Liu XS, Ahringer J (2009). **Differential chromatin marking of introns and expressed exons by H3K36me3.** *Nature Genetics* **41:**376-381.
https://doi.org/10.1038/ng.322

Konieczny P, Stepniak-Konieczna E, Sobczak K (2014). **MBNL proteins and their target RNAs, interaction and splicing regulation**. *Nucleic Acids Research* **42**:10873-10887.
https://doi.org/10.1093/nar/gku767

Konieczny P, Stepniak-Konieczna E, Sobczak K (2018). **MBNL expression in autoregulatory feedback loops.** *RNA Biology* **15**: 1-8.
https://doi.org/10.1080/15476286.2017.1384119

Korb E, Herre M, Zucker-Scharff I, Gresack J, Allis CD, Darnell RB (2017**). Excess translation of epigenetic regulators contributes to Fragile X Syndrome and is alleviated by Brd4 inhibition.** *Cell* **170:**1209-1223.
https://doi.org/10.1016/j.cell.2017.07.033

Li R, Dong Q, Yuan X, Zeng X, Gao Y, Chiao C, et al. (2016). **Misregulation of alternative splicing in a mouse model of Rett syndrome.** *PLoS Genetics* **12**:e100612.
https://doi.org/10.1371/journal.pgen.1006129

Li M, Shin J, Risgaard RD, Parries MJ, Wang J, Chasman D, Liu S, Roy S, Bhattacharyya A, Zhao X (2020). **Identification of FMR1-regulated molecular networks in human neurodevelopment.** *Genome Research* **30**:361-374.
https://doi.org/10.1101/gr.251405.119

Maurin T, Lebrigand K, Castagnola S, Paquet A, Jarjat M, Popa A, Grossi M, Rage F, Bardoni B. (2018). **HITS-CLIP in various brain areas reveals new targets and new modalities of RNA binding by fragile X mental retardation protein.** *Nucleic Acids Research* **46**:6344-6355.
https://doi.org/10.1093/nar/gky267

Osterweil EK, Chuang SC, Chubykin AA, Sidorov M, Bianchi R, Wong RK, Bear MF (2013) **Lovastatin corrects excess protein synthesis and prevents epileptogenesis in a mouse model of fragile X syndrome.** *Neuron* **77**:243-250.
https://doi.org/10.1016/j.neuron.2012.01.034

Parras A, Anta H, Santos-Galindo M, Swarup V, Elorza A, Nieto-González JL, Picó S, Hernández IH, Díaz-Hernández JI, Belloc E, Rodolosse A, Parikshak NN, Peñagarikano O, Fernández-Chacón R, Irimia M, Navarro P, Geschwind DH, Méndez R, Lucas JJ (2018). **Autism-like phenotype and risk gene mRNA deadenylation by CPEB4 mis-splicing.** *Nature* **560**:441-446.
https://doi.org/10.1038/s41586-018-0423-5

Paz, I., Kosti, I., Ares Jr, M., Cline, M., & Mandel-Gutfreund, Y. (2014). **RBPmap: a web server for mapping binding sites of RNA-binding proteins.** *Nucleic acids research*, ***42***: W361-W367.
https://doi.org/10.1093/nar/gku406

Pradeepa MM, Sutherland HG, Ule J, Grimes GR, Bickmore WA (2012). **Psip1/Ledgf p52 binds methylated histone H3K36 and splicing factors and contributes to the regulation of alternative splicing.** *PLoS Genetics* **8**:e1002717**.** https://doi.org/10.1371/journal.pgen.1002717

Richter JD, Coller J (2015). **Pausing on polyribosomes: make way for elongation in translational control.** *Cell* **163:**292-300. https://doi.org/10.1016/j.cell.2015.09.041

Richter JD, Zhao X. (2021) **The molecular biology of FMRP: new insights into fragile X syndrome.** *Nature Reviews Neuroscience* **22**:209-222. https://doi.org/10.1038/s41583-021-00432-0

Santoro MR, Bray SM, Warren ST (2012) **Molecular mechanisms of fragile X syndrome: a twenty-year perspective**. *Annual Review of Pathology* **7**:219-245. https://doi.org/10.1146/annurev-pathol-011811-132457

Sawicka K, Hale CR, Park CY, Fak JJ, Gresack JE, Van Driesche SJ, Kang JJ, Darnell JC, Darnell RB (2019). **FMRP has a cell-type-specific role in CA1 pyramidal neurons to regulate autism-related transcripts and circadian memory.** *Elife* **8**:e4691. https://doi.org/10.7554/eLife.46919

Schwartz S, Meshorer E, Ast G (2009). **Chromatin organization marks exon-intron structure.** *Nature Structural and Molecular Biology* **16**:990-995. https://doi.org/10.1038/nsmb.1659

Shah S, Molinaro G, Liu B, Wang R, Huber KM, Richter JD (2020**). FMRP control of ribosome translocation promotes chromatin modifications and alternative splicing of neuronal genes linked to autism.** *Cell Reports* **30**:4459-4472. https://doi.org/10.1016/j.celrep.2020.02.076

Shah S, Richter JD (2021). **Do fragile X syndrome and other intellectual disorders converge at aberrant pre-mRNA splicing?** *Frontiers in Psychiatry* **12**:715346. https://doi.org/10.3389/fpsyt.2021.715346

Shen, S., Park, J.W., Lu, Z., Lin, L., Henry, M.D., Wu, Y.N., Zhou, Q., and Xing, Y. (2014). **rMATS: Robust and flexible detection of differential alternative splicing from replicate RNA-Seq data.** Proc. Natl. Acad. Sci. 111, E5593-E5601. https://doi.org/10.1073/pnas.1419161111

Shu H, Donnard E, Liu B, Jung S, Wang R, Richter JD (2020). **FMRP links optimal codons to mRNA stability in neurons.** *Proceedings of the National Academy of Sciences U S A.* **117**:30400-30411. https://doi.org/10.1073/pnas.2009161117

Spector DL, Lamond AI (2011). **Nuclear speckles.** *Cold Spring Harbor Perspectives in Biology* **3**:a000646. https://doi.org/10.1101/cshperspect.a000646

Stefani G, Fraser CE, Darnell JC, Darnell RB (2004). **Fragile X mental retardation protein is associated with translating polyribosomes in neuronal cells.** *Journal of Neuroscience* **24:**7272-7276.
https://doi.org/10.1523/JNEUROSCI.2306-04.2004

Tamanini F, Bontekoe C, Bakker CE, van Unen L, Anar B, Willemsen R, Yoshida M, Galjaard H, Oostra BA, Hoogeveen AT (1999). **Different targets for the fragile X-related proteins revealed by their distinct nuclear localizations.** *Human Molecular Genetics* **8**:863-869.
https://doi.org/10.1093/hmg/8.5.863

Tapial J, Ha KCH, Sterne-Weiler T, Gohr A, Braunschweig U, Hermoso-Pulido A, Quesnel-Vallières M, Permanyer J, Sodaei R, Marquez Y, Cozzuto L, Wang X, Gómez-Velázquez M, Rayon T, Manzanares M, Ponomarenko J, Blencowe BJ, Irimia M (2017). **An atlas of alternative splicing profiles and functional associations reveals new regulatory programs and genes that simultaneously express multiple major isoforms.** Genome Research **27**:1759-1768.
https://doi.org/10.1101/gr.220962.117

Terenzi F, Ladd AN. (2010) **Conserved developmental alternative splicing of muscleblind-like (MBNL) transcripts regulates MBNL localization and activity**. *RNA Biology* **7**:43-55.
https://doi.org/10.4161/rna.7.1.10401

Thacker S, Sefyi M, Eng C (2020). **Alternative splicing landscape of the neural transcriptome in a cytoplasmic-predominant Pten expression murine model of autism-like behavior.** *Translational Psychiatry* **10**:380.
https://doi.org/10.1038/s41398-020-01068-x

Tran SS, Jun HI, Bahn JH, Azghadi A, Ramaswami G, Van Nostrand EL, Nguyen TB, Hsiao YE, Lee C, Pratt GA, Martínez-Cerdeño V, Hagerman RJ, Yeo GW, Geschwind DH, Xiao X (2019). **Widespread RNA editing dysregulation in brains from autistic individuals.** *Nature Neuroscience 22*:25-36.
https://doi.org/10.1038/s41593-018-0287-x

Tran H, Gourrier N, Lemercier-Neuillet C, Dhaenens CM, Vautrin A, Fernandez-Gomez FJ, Arandel L, Carpentier C, Obriot H, Eddarkaoui S, Delattre L, Van Brussels E, Holt I, Morris GE, Sablonnière B, Buée L, Charlet-Berguerand N, Schraen-Maschke S, Furling D, Behm-Ansmant I, Branlant C, Caillet-Boudin ML, Sergeant N (2011). **Analysis of exonic regions involved in nuclear localization, splicing activity, and dimerization of Muscleblind-like-1 isoforms.** *Journal of Biological Chemistry* **286:**16435-16446.
https://doi.org/10.1074/jbc.M110.194928

Udagawa T, Farny NG, Jakovcevski M, Kaphzan H, Alarcon JM, Anilkumar S, Ivshina M, Hurt JA, Nagaoka K, Nalavadi VC, Lorenz LJ, Bassell GJ, Akbarian S, Chattarji S, Klann E, Richter JD (2013). **Genetic and acute CPEB1 depletion ameliorate fragile X pathophysiology.** *Nature Medicine* **19:1473-1477.**
https://doi.org/10.1038/nm.3353

Wu T, Hu E, Xu S, Chen M, Guo P, Dai Z, Feng T, Zhou L, Tang W, Zhan L, Fu x, Liu S, Bo X, Yu G (2021). **"clusterProfiler 4.0: A universal enrichment tool for interpreting omics data."** *The Innovation*, 2(3), 100141.
https://doi.org/10.1016/j.xinn.2021.100141

927 Yu G, Wang L, Han Y, He Q (2012). **"clusterProfiler: an R package for comparing biological**
928 **themes among gene clusters."** *OMICS: A Journal of Integrative Biology*, 16(5), 284-287.
929 https://doi.org/10.1089/omi.2011.0118
930
931 Yukselen O, Turkyilmaz O, Ozturk AR, Garber M, Kucukural A (2020). **DolphinNext: a**
932 **distributed data processing platform for high throughput genomics.** *BMC Genomics*.
933 **21**:310.
934 https://doi.org/10.1186/s12864-020-6714-x
935
936
937

Additional files

Supplementary file 1. RNA-seq analysis of gene expression in WT and *Fmr1* KO mice and siNT and siFmr1 treated N2A cells.

Differential gene expression analysis of WT and *Fmr1* KO tissues from CTX, HC, CB, LV, MU, TE and N2A cells.

Supplementary file 2. Alternative splicing events in WT and *Fmr1* KO mice cortex (CTX).

Supplementary file 3. Alternative splicing events in WT and *Fmr1* KO mice hippocampus (HC).

Supplementary file 4. Alternative splicing events in WT and *Fmr1* KO mice cerebellum (CB).

Supplementary file 5. Alternative splicing events in WT and *Fmr1* KO mice liver (LV).

Supplementary file 6. Alternative splicing events in WT and Fmr1 KO mice muscle (MU).

Supplementary file 7. Alternative splicing events in WT and *Fmr1* KO mice testis (TE).

Supplementary file 8. Alternative splicing events in siNT and siFmr1 treated N2A cells.

Supplementary file 9. MBNL1 binding motif analysis in N2A cells.